629

THE JOHN CRERAR NOV 25 1941 LIBRARY

JOURNAL OF THE AERONAUTICAL SCIENCES

VOLUME 9 NOVEMBER, 1941 NUMBER 1

Published in three Sections—Section One

CONTENTS

Determination of Strain Distribution by the Photo-Grid Process . . . . . GIVEN A. BREWER AND ROBERT B. GLASSCO 1

Theoretical Correction for the Lift of Elliptic Wings . . . . . ROBERT T. JONES 8

On Propeller-Tip Interference Due to the Proximity of a Fuselage . . . . . ALBERT GAIL AND HO-SHEN LU 11

An Approximate Method to Predict the Transition or "Flare" Flight Path in the Take-off or Landing of an Airplane . . . . . OMER WELLING 17

Airplane Vibration Tests as Related to the Flutter Problem . . . . . CHARLES B. LYMAN 24

Institute Notes 31

Published by the

INSTITUTE OF THE AERONAUTICAL SCIENCES INC.

JOURNAL OF THE AERONAUTICAL SCIENCES

VOL. 9 NOVEMBER, 1941 NO. 1

Editors: HUGH L. DRYDEN, *Chief of Mechanics and Sound Division, National Bureau of Standards*
J. C. HUNSAKER, *Coordinator of Research and Development, Navy Department (on leave of absence for the emergency)*

PUBLISHED MONTHLY BY THE INSTITUTE OF THE AERONAUTICAL SCIENCES INC.
AT 20TH AND NORTHAMPTON STS., EASTON, PA.

The JOURNAL OF THE AERONAUTICAL SCIENCES is the official publication of the Institute of the Aeronautical Sciences Inc., and prints papers of scientific and technical interest to members and subscribers. In general, it provides an opportunity for specialists to publish articles disclosing new knowledge and new applications in the field of the aeronautical sciences. The Journal restricts itself to the aeronautical aspects of advances in science and engineering, and papers printed have either been submitted directly to the Journal or have been previously presented at a meeting of the Institute. News of the Institute is furnished members through the Journal.

The AERONAUTICAL REVIEW, which is published both as a section and separately as an edition of the Journal of the Aeronautical Sciences, keeps members and subscribers informed regarding the contents of new books and current periodicals in the field of aeronautics. It reviews new developments in the aircraft industry appearing in house organs and catalogues published by aircraft and engine manufacturers and other companies engaged in aeronautical activities.

Statements and opinions expressed in the Journal or the Aeronautical Review are to be understood as individual expressions of the authors, and not those of the Institute.

SUBSCRIPTION RATES

Journal of the Aeronautical Sciences including the Aeronautical Review Section

United States and Possessions		Foreign Countries, Including Canada (American Currency Rates)	
1 Year	$10.00	1 Year	$12.50
Single Copies	1.00	Single Copies	1.25

Journal of the Aeronautical Sciences—Aeronautical Review Edition Only

United States and Possessions		Foreign Countries, Including Canada (American Currency Rates)	
1 Year	$2.50	1 Year	$3.00
Single Copies	.25	Single Copies	.30

Manuscripts for publication, proofs, and all correspondence should be addressed to the Editorial Secretary of the Journal.

Correspondence regarding subscriptions may be addressed to Publication Office, 20th and Northampton Sts., Easton, Pa., or to the Editorial Office of the JOURNAL OF THE AERONAUTICAL SCIENCES, 1505 RCA Building West, 30 Rockefeller Plaza, New York, New York. Cable address: INSAEROSCI.

Entered as Second Class Matter at the Post Office, Easton, Pa., May 1, 1937. Acceptance for mailing at a special rate of Postage provided for in the Act of August 24, 1912. Authorized April 29, 1937.

JOURNAL OF THE AERONAUTICAL SCIENCES

VOLUME 9 . NOVEMBER, 1941 NUMBER 1

Determination of Strain Distribution by the Photo-Grid Process

GIVEN A. BREWER AND ROBERT B. GLASSCO

*Lockheed Aircraft Corporation**

ABSTRACT

The purpose of this paper is to describe the photo-grid process, a new method of measuring local deformations. The process consists of photographing a pattern of lines upon a sensitized specimen which is then tested and the amount of deformation determined by measuring the new spacing of the lines. Gage lengths as small as 0.01 inch are used. By this process the strain distribution in tensile specimens of aluminum alloys has been plotted; also the strains produced by several forming operations have been determined. The maximum local elongation measured in tensile test specimens is much higher than the average in two inches and is indicative of the elongations obtained in forming operations of simple bending or stretching. In deep drawn shells even higher strains were measured. The phenomenon of progressive strain hardening with reference to the strain distribution found in the tensile test specimens is discussed.

INTRODUCTION

STUDIES OF elongation and ductility of metals and alloys have in the past been confined to results measured over comparatively long intervals such as the two-inch and eight-inch gage lengths customarily used in tensile strength tests. It has been recognized that within such gage lengths the elongation may be distributed in a non-uniform manner, and that consequently, the measured overall percentage elongation will vary with the gage length used. Such an analysis is of prime importance in approaching all types of forming problems in which the failure of the metal at some critical section is the limiting factor. Yet a survey of the existing literature reveals that the subject has received little attention.

In one of the publications[1] Crane merely alludes to the fact that the local elongation at the point of failure is much greater than the "general" elongation in a two-inch gage length. In an earlier paper[2] Krivobok, Lincoln, and Patterson treat this subject more fully; their studies were confined to stainless steels of pseudo-austenitic character and are shown in the form of curves of *distribution* of elongation over standard two-inch gage lengths (Fig. 1). The effect of strain hardening properties on the distribution of local elongations is brought out in this reference, and will be given further attention later on in the present paper. Elam[3] is primarily concerned with the phenomenon whereby the elongation in some materials during the tensile test is assumed to occur by what may be termed "small jumps" rather than uniformly. True, reference is made to the non-uniformity of strain distribution throughout the specimen under test, but because the method of observation was quite cumbersome, detailed data were not obtained. Templin and Sturm[4] show the variation in overall elongation when the gage lengths are increased from one inch to ten inches. Shorter gage lengths were not studied and, therefore, their studies do not contain information pertaining to what may be called "local distribution" of elongation in tensile testing.

It seems clear that the limitation on previous work

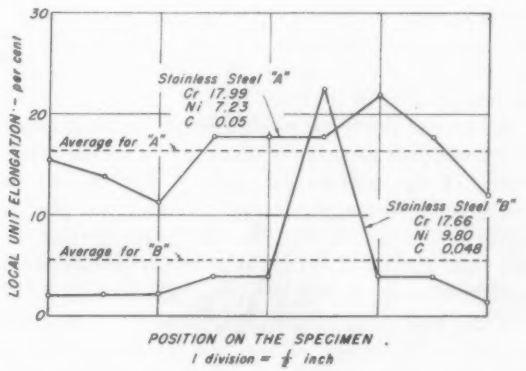

FIG. 1. Distribution of elongation, measured every quarter inch, over two-inch gage lengths for two austenitic stainless steels, both cold-rolled to about 165,000 pounds per square inch.[2]

Received August 19, 1941.

* Structures Research Laboratory

L629.051
J82
670691

has been partly caused by the lack of a suitable technique to investigate the local elongations. Experiments which may be made to determine the local elongation by measuring the reduced cross-sectional area show only part of the picture and are limited in application. Even the recently developed electric strain gage is not adapted to measurements over extremely small intervals.

It is, therefore, the purpose of the present paper to describe a new method, the photo-grid process, now being used at the Lockheed Aircraft Corporation for measuring local deformations, and for studying the ultimate significance thereof in the technical study of metal forming.

Technique Developed in Present Investigation

The experimental technique which is being used in the present investigation was developed by Given A. Brewer of the Lockheed Aircraft Corporation. Briefly, the technique consists of photographing a pattern of lines upon a sensitized specimen which is then tested and the amount of deformation determined by measuring the new spacing of the lines.

In order to produce the photograph on the specimen, a high-contrast negative is first made from the original source of the pattern or grid. A very satisfactory source for a rectangular coordinate grid is a photoengraver's glass screen with parallel diamond-ruled lines 0.01 inch apart. A tensile coupon prepared with this pattern is shown in Fig. 2. Other sources such as rectangular and polar graph paper have been used satisfactorily. Examples of the use of these two grid sources are shown in Fig. 3 and Fig. 4, respectively.

Following the preparation of the negative, the surface of the test specimen is sensitized, and on the sensitized surface a contact print of the grid is made. A detailed description of this printing process is given in the Appendix.

For examination of the tested specimen, a cathetometer or measuring microscope is generally used. Occasionally, it is desirable to make a photo-enlargement of the deformed grid and to measure the strain with a scale and dividers. This applies to cases in which the specimen will not fit in the cathetometer. In these latter cases an undeformed "control" area is photographed in the same picture with the specimen in order to establish the scale.

The special advantages of the technique described above are as follows: (1) the printing process eliminates all scratches and gage marks which might give stress concentrations; (2) the line pattern makes it possible to determine the unit deformation of a very small length; (3) the use of the engraver's screen and the methods of magnification give good accuracy; (4) two-dimensional deformation is shown which is important in many cases; (5) the method can be applied to any odd-shaped specimen as long as a contact print can be made on it before it is deformed; and (6) relatively small expense is incurred, whether for large, small, or odd-shaped specimens.

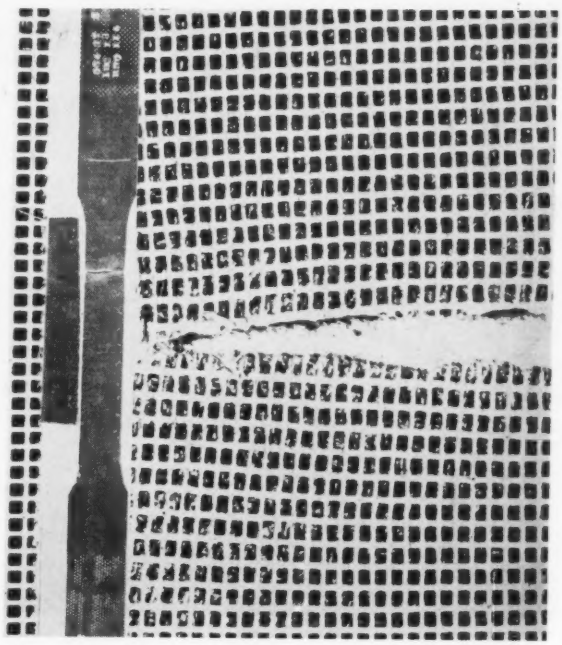

Fig. 2. Photographic enlargement of a tested tensile coupon made of 24S-T Alclad sheet, 0.064 inch in thickness, with a 0.01-inch rectangular photo-grid on one surface.

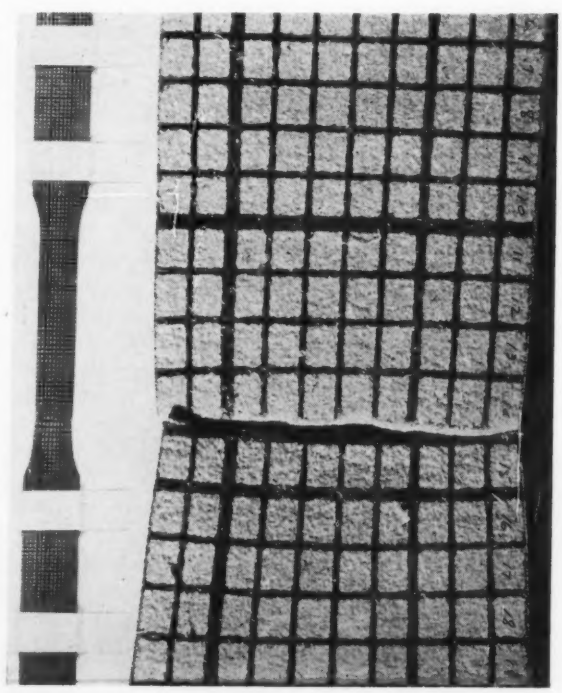

Fig. 3. Photographic enlargement of a tested tensile coupon made of 24S-T Alclad sheet, 0.064 inch in thickness, with a 0.05-inch rectangular photo-grid on one surface.

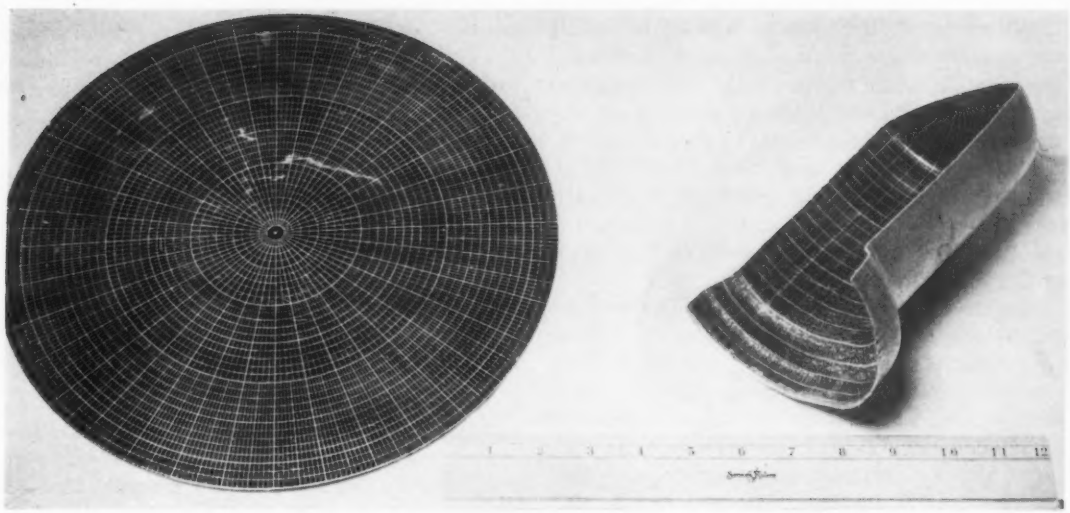

FIG. 4. Deep drawn shell and blank of 24S-O Alclad with a polar photo-grid.

RESULTS OF TESTS USING THE PHOTO-GRID

Tensile Tests

The first application of the photo-grid was on standard sheet metal tensile coupons. Fig. 2, already mentioned, shows a typical aluminum alloy tensile specimen on which was imprinted a grid made up from the photo-engraver's screen having lines spaced 0.01 inch apart. The same illustration shows an enlargement of the section of the specimen adjacent to the rupture. It is to be noted that the photographic enlargement shows very clearly the details in the area adjacent to rupture. Fig. 3 shows a specimen on which was used a grid produced with graph paper having 0.05-inch squares. By measuring the local unit elongation or strain along the length of these specimens, as already described, a strain distribution curve was plotted. In Figs. 5 and 6 are shown the curves plotted for the specimens illustrated in Figs. 2 and 3. Measurements for these curves were made every 0.02 inch and 0.05 inch, respectively.

Each point plotted for the above strain distribution curves has an abscissa corresponding to the position on the undeformed specimen of a small finite increment of length as measured from some arbitrary reference axis. It has an ordinate equal to the unit elongation (strain) of this increment of length as measured from the photograph.

When a curve is drawn through the points, each ordinate then represents unit elongation for a differential

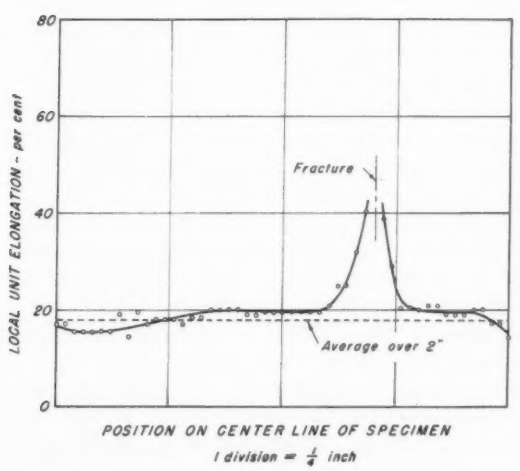

FIG. 5. Distribution of elongation, measured for 0.02-inch gage lengths, on the 24S-T Alclad specimen shown in Fig. 2.

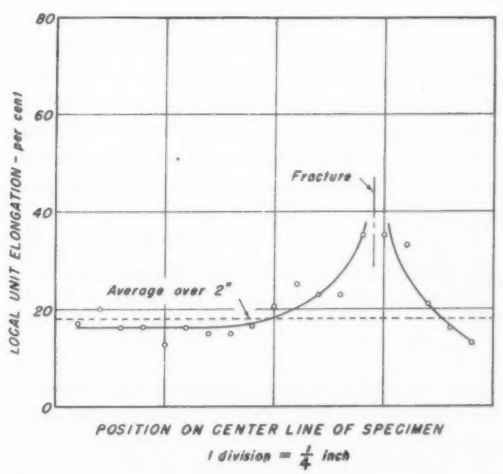

FIG. 6. Distribution of elongation, measured for 0.05-inch gage lengths, on the 24S-T Alclad specimen shown in Fig. 3.

length of specimen at that location; and the area under the curve, being the summation of the elongations of each differential length, represents the *total* elongation of the specimen. The area under the curve divided by the original length of the specimen then represents the *average* unit elongation, or *average* strain, over the entire specimen. This last is the quantity usually determined in tensile tests using long gage lengths and is commonly expressed as the "per cent elongation" of the material.

The specimens used as illustrations in this report are merely samples taken from the large number of 24S-O and 24S-T Alclad aluminum alloys,* specimens which have been tested. As might have been expected, there has been a large variation in the strain distribution curves of the specimens tested; no two are exactly alike. However, from the practical standpoint the elongation over a short gage length appears important, especially in forming small bends, etc. Therefore, data have been compiled from many specimens, based on the strain distribution curves and showing the elongation in $^1/_4$ inch and 0.01 inch, as well as in the standard 2 inches. These data show the following ranges of values:

Material	2 Inches	$^1/_4$ Inch	0.01 Inch
24S-O Alclad	10–22%	25–45%	31–71%
24S-T Alclad	16–21%	25–35%	44–62%
24S-T Alclad, purchased as 24S-O and heat treated by various methods	10–22%	20–40%	27–65%

The curves discussed above have shown clearly the non-uniform character of the strain distribution throughout a specimen when the latter has been pulled to failure. What occurs prior to failure has been observed by taking a series of photographs during the pulling of a specimen. These photographs show that the pronounced peak in the strain distribution curve does not appear until the load is approximately at a maximum. The results also show, as might have been predicted, that the failure occurs at the location of maximum strain, providing that there is no interference from extraneous sources. Even though the increments of length over which the elongations are measured are sufficiently small to show quite accurately the possible extent of strain in the alloys under investigation, the maximum elongation at the infinitesimal point of failure, which might be called the "ultimate strain," cannot be determined.

Deep Drawing Tests

The photo-grid has been successfully applied to tests of deep drawing. By using a polar coordinate grid, measurements were made of both the radial stretching and circumferential shrinking occurring over the entire surface of the shells. Because of the favorable system of combined stresses which occurs in this particular forming operation, very high strains are obtainable. With 24S-O Alclad shells drawn in three stages compressive strains of 60 per cent and tensile strains of 110 per cent were obtained without intermediate annealing. In Fig. 4 is illustrated one of these specimens—first, the unformed blank printed with the polar grid, and second, the final shell after three draws.

Dimpling Tests

The photo-grid is being used in a study of the dimpling of sheet aluminum parts. This process of flanging a rivet hole, when a flush rivet or screw is to be used, stretches the rim of the hole. By printing a photo-grid of miniature polar coordinates concentrically with the hole as illustrated in Fig. 7, the elongations produced by both the impact and the squeeze type dimpling tools have been measured. The range of elongations obtained in 24S-T Alclad purchased as 24S-O and heat treated was found to be from 20 per cent to 32 per cent. Maximum permissible values of elongation for this forming process are not yet determined, but it is interesting to note that these values obtained thus far are considerably higher than the average in two inches obtained in standard tensile specimens.

Bending Large Extrusions

The photo-grid was used for making elongation measurements on a large 24S-T aluminum alloy extrusion which had been cracking during a bending operation. The measurements showed that this bending operation produced a maximum stretching of only 13 per cent in the outer fibers. Further measurements showed that material of normal ductility (*i.e.*, capable of about $16^1/_2$ per cent elongation over a two-inch gage length when pulled as a standard tensile coupon) could successfully withstand a stretching of at least 22 per cent when being bent. Consequently, the basic cause of the cracking was traced to a portion of the extrusions having subnormal ductility, a result of a work-hardened condition along the outer portion which happened to be subjected to the greatest stretching.

In connection with the above study, the measurements showed how the actual stretching in a bend compares with the theoretically required elongation calculated from the bend radius and the location of the neutral surface. The calculated elongation for the above case was 26 per cent; whereas the actual maximum elongation for a 9 degree bend was 13 per cent, and for a 30 degree bend, 22 per cent.

This investigation demonstrated clearly the practical importance of a careful study of permissible elongations in connection with the design and tooling of curved parts.

* 24S Alclad has chemical make-up as follows; 4.5% Cu, 0.6% Mn, 1.5% Mg, remainder Al, and with a pure aluminum coating. "O" refers to annealed (soft) temper; "T" refers to solution heat-treated and aged (hard) temper.

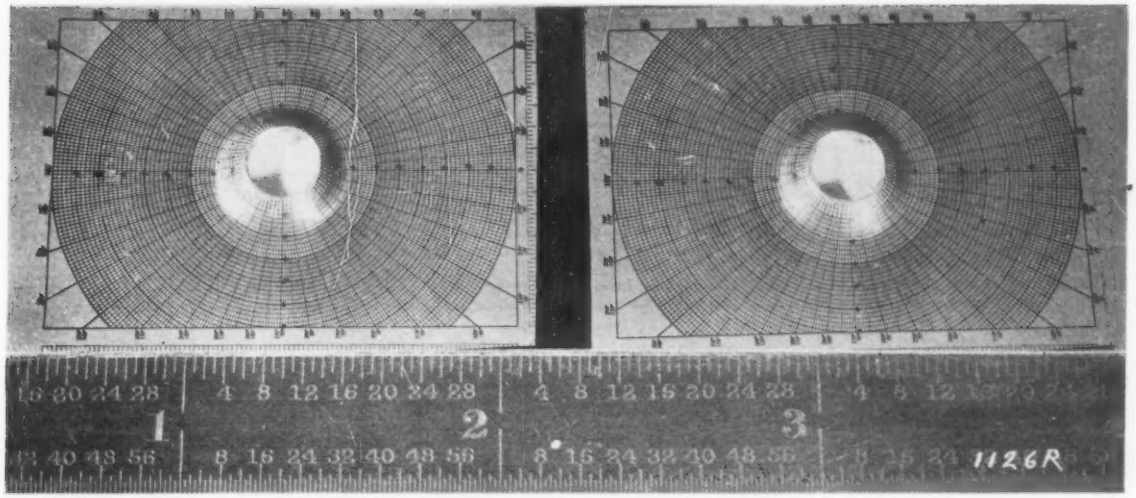

FIG. 7. Dimple specimens with a polar photo-grid.

DISCUSSION

To understand the non-uniformity of strain distribution occurring in tensile specimens as illustrated by the curves already shown, it must be recognized, that, because of the nature of the physical structure of the metal, the tensile stress at which yielding begins is not exactly the same at every point in the specimen. Furthermore, the cross-sectional area is not uniform because of the difficulty of securing absolutely accurate dimensions. Consequently, at some location in the specimen the yield resistance, which may be defined as the product of area and yield stress, will be a minimum. Under the application of a certain load localized yielding first occurs at this location. Accompanying the stretching is a reduction of the cross-sectional area which further weakens this section of the specimen. Whether the elongation will continue to be concentrated at this location, leading ultimately to failure here, or whether it will be subsequently distributed in the rest of the specimen before failure occurs, depends upon the ability of the material to *increase* its yield resistance at the first instant of plastic flow.

As is well known, practically all metallic alloys, and even metals, have the faculty of strain hardening, but of widely different magnitude. If the material being loaded has an appreciable capacity for strain hardening, and if sufficient time is allowed for this phenomenon to take place, the reduction of the cross-sectional area at the original point of yield (resulting in an *increase* in stress per unit area) is partially compensated by an actual increase in the unit resistance of the material. The magnitude of the strain hardening may even be sufficient to make the section at which the original yielding occurred *stronger* than the rest of the specimen, thus temporarily halting yielding of the metal at this point. At the next instant the same process will take place in some other section where again the yield resistance is less than the applied load. This cycle is repeated until the rate of strain hardening relative to elongation and the rate of area reduction relative to elongation are such that the strength of some section no longer increases with further stretching. When this condition is reached, the local necking down will occur and failure is rapidly brought about. Thus, as a result of strain hardening, considerable stretching may take place at sections which do not break, and a higher *average* elongation is obtained before the specimen fails. The shape of the strain distribution curve will obviously be different in the two cases.

The above explanation was offered by Krivobok, *et al.*, in their paper already referred to.[2] Their studies and observations were made on samples of stainless steels, in which the degree of physico-chemical instability of the alloys, influenced by variations in analysis, was found to be the cause of marked differences in local strain and its distribution in tensile specimens studied. In Fig. 1, for example, it is shown that the low-nickel stainless steel "A," having pronounced work-hardening properties, shows a much higher *average* elongation (although the same *peak* elongation) as the high-nickel stainless steel "B," which does not exhibit the same degree of strain hardening.

No phase change is involved in the hardening of aluminum alloys, however; and hence physico-chemical instability does not enter into the results. It might be expected, therefore, that the strain distribution in aluminum alloys would differ from that found in certain stainless steels. Comparison of Fig. 5 or Fig. 6 with Fig. 1 indicates that the shape of the strain distribution curve for 24S-T Alclad does indeed differ from that for stainless steel "A" (the strain-hardening steel). It is quite similar, however, to that of stainless

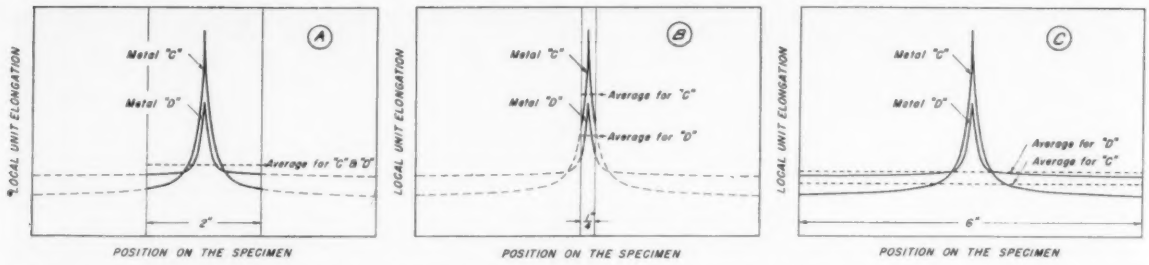

FIG. 8. Distribution of elongation over six-inch gage lengths in two imaginary metals. (*A*) With the average unit elongation in two inches shown. (*B*) Average unit elongation in one-quarter inch shown. (*C*) Average unit elongation in six inches shown.

steel "B" (the non-strain-hardening steel). This agrees with the general knowledge that 24S-T exhibits a relatively slight tendency to strain hardening.

In a general way, the information presented herein leads to the following important conclusions: first, it can be seen that for a given material the average unit elongation measured after failure is very dependent upon the gage length over which it is measured. Second it is evident that the customary method of evaluating the ductility of a metal, that is, measuring the average unit elongation over a standard gage length of say two inches, gives a very incomplete picture. It is the *shape* of the strain distribution curve which is of vital importance in the study of the forming properties of a material.

To study further the significance of the shape of the strain distribution curve, consider two imaginary metals, "C" and "D," with the same average strain over two inches, but with different maximum local strains. Fig. 8*A* shows the strain distribution curves of these metals with the two-inch gage length outlined to show the same average over this length for both curves. If the length of material being measured is less than two inches, say one-quarter of an inch, the average elongation of Metal "C" is greater than that of Metal "D," as shown in Fig. 8*B*. On the other hand, for a gage length greater than two inches, say six inches, Metal "D" has a higher average elongation as shown in Fig. 8*C*. Curves showing average elongation *vs.* gage length for these two metals are given in Fig. 9.

The fact that the material can actually sustain high local elongations of magnitude corresponding to the peak of the distribution curve, accounts for the fact that in sharp bends where elongation is confined to a short distance, high strains are found to exist. Such strains are often considerably higher than one would be led to believe possible on the basis of the allowable elongations determined over a two-inch gage length.

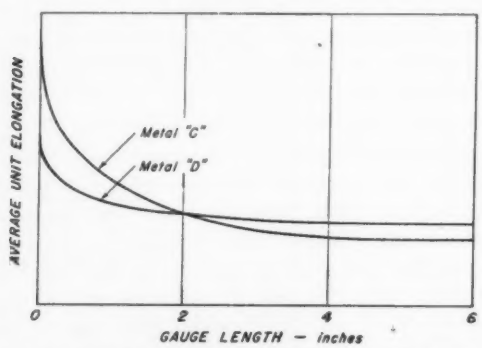

FIG. 9. Variations of average unit elongation with gage length for metals *C* and *D* from Fig. 8.

It has been found that the average elongation taken over a one-quarter-inch gage length on the peak of the distribution curve gives a good indication of the relative permissible minimum bend radii of various aluminum alloy sheets. On the other hand, little or no prediction of minimum bend radii can be made on the basis of the elongations in two-inch gage lengths.

PROGRAM OF FUTURE WORK

It is the desire of the authors that this article be considered an invitation to other research engineers to adapt the photo-grid technique to the many types of experimental work and testing where it can be used to advantage. Future work to be conducted using the photo-grid should consist of: (1) obtaining strain distribution curves on the materials commonly subject to forming and other plastic deformation. These curves should cover conditions existing throughout the plastic range, as well as close to failure; (2) further study of the strain hardening phenomenon in relation to the strain distribution curves; (3) study of crystal and atomic structure as related to the phenomena of strain hardening and strain distribution; (4) application of the knowledge gained above to practical problems of forming; and (5) application of the photo-grid technique to these problems of plastic deformation.

APPENDIX

DETAILED DESCRIPTION OF THE PRINTING PROCESS

In the photo-grid process the printing of the line pattern onto the specimen is done photographically. The main procedures in the printing process are as follows: the specimen to be printed is first cleaned with pumice and cold water, after which is applied to the surface a sensitizing solution consisting of 28 parts by weight of water, 4 parts of photoengraving glue, 1 part of ammonium bichromate, and $^1/_4$ part of ammonia water.

(This sensitizing solution was a development of Charles W. Miller of the Lockheed Aircraft Corporation.) If the specimen is a large plate, it is placed on a regular photo-engraving plate-whirl consisting of a turn-table rotating in warm air, and the solution is poured on. If the specimen has an irregular shape, or is too large for the plate-whirl, the solution is sprayed on with an air gun using 15 pounds per square inch pressure. For spraying, 1 ounce of stock solution is dissolved in 4 ounces of water and 4 ounces of alcohol.

As soon as the surface of the metal has been prepared, the negative is placed face to face with the sensitized surface and exposed for 5 minutes in a vacuum frame at a distance of about 36 inches from a 35 ampere arc light. Following the exposure, the specimen is rinsed with cold water and a solution of Diamond dye (one box of Wells and Richardson dye mixed with one pint of water) is applied and allowed to dry for 5 minutes, after which the specimen is rinsed with cold water and again allowed to dry before it is ready for testing.

References

[1] Crane, E. V., *Plastic Working of Metals and Power-Press Operations*, Second Edition, page 22, John Wiley and Sons, Inc., New York, N. Y., 1939.

[2] Krivobok, V. N., Lincoln, R. A., and Patterson, R., Jr., *Austenitic Stainless Alloys—Their Properties and Characteristics*, Transactions, Am. Soc. for Metals, Vol. 25, No. 3, pages 668–677, 1937.

[3] Elam, C. F., *Non-Uniform Yielding in Metals During a Tensile Test*, Engineering, pages 325–327, March 29, 1940.

[4] Templin, R. L., and Sturm, R. G., *Some Stress-Strain Studies of Metals*, Journal of the Aeronautical Sciences, Vol. 7, No. 5, pages 189–198, March, 1940.

Theoretical Correction for the Lift of Elliptic Wings

ROBERT T. JONES†

National Advisory Committee for Aeronautics

In the wing section theory the magnitude of the circulation, and hence of the lift, is determined by the velocity that would be induced near the trailing edge of the section in a non-lifting potential flow. In three-dimensional flow the problem is complicated by the presence of the wake and no simple basic solution has been found. Treatment of the problem of a wing of finite span has therefore been on the basis of the two-dimensional theory, corrected for the effect of the wake.*

The correction commonly applied is that introduced by Prandtl and known as the lifting-line theory. The downflow induced by the wake is considered, in this theory, to reduce the relative normal velocity and hence the edge velocity of the wing. It is assumed, however, that once the true angle of attack is determined for any section of the wing its effect in producing circulation and lift is the same as in two-dimensional flow. This assumption is expressed by the equation

$$C_L = 2\pi(\alpha - \alpha_i) \tag{1}$$

where 2π is the slope of the lift curve for the thin wing of infinite aspect ratio, α is the angle of attack of the section, and α_i is the induced angle of downflow.

Eq. (1) takes into account the effect of the wake in diminishing the relative normal velocity of the wing. A further correction is indicated by the fact, established in hydrodynamic theory, that the surface velocities induced by a given relative motion of a body in three-dimensional flow are generally smaller than those in two. For example, the maximum, or "edge" velocity around an infinite cylinder is 1, while that around a sphere of the same cross-section is $1/2$. Similarly, if the velocity around the edge of an endless thin plate is taken as unity, the corresponding velocity around the edge of a circular disc is found to be $2/\pi$, or 0.637.

In the case of an elliptic disc the velocity at every point is reduced by the factor $1/E$, where E is the ratio of the semiperimeter of the ellipse to the span. (See appendix.) Further investigation shows that the chordwise cross-sections of the non-lifting potential flow are similar all along the span of the elliptic plate and are the same as those obtained from the wing-section theory except for this constant reduction factor.

Received July 31, 1941.

† Assistant Aeronautical Engineer.

* More recently the problem has been treated on the basis of the acceleration potential, which vanishes in the wake.[1] The method is still one of considerable difficulty, however.

If the velocity distributions of the circulatory flow are also assumed to be similar to those given by the wing-section theory, the circulation required to satisfy the Kutta condition at each section should be reduced by the same factor. The corrected formula for the lift is then

$$C_L = (2\pi/E)(\alpha - \alpha_i) \tag{2}$$

This correction may be given a physical interpretation by considering that a finite wing offers a longer edge around which the air may escape (see Fig. 1),

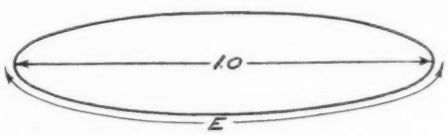

Fig. 1. Correction factor E for the effect of the perimeter ratio on the lift: $C_L = (2\pi/E)(\alpha - \alpha_i)$.

and that the air velocities are therefore less in the proportion that the length of the edge is greater. The rule is not exact for plan forms other than the elliptical.

Since the velocity of the non-lifting potential flow is constant all around the edge of the elliptic plate, the circulation required will be proportional to the chord at each section. The circulation is thus elliptically distributed spanwise. Such a distribution, with the chordwise distribution assumed earlier, leads, as in the lifting-line theory, to the relation

$$\alpha_i = C_L/\pi A \tag{3}$$

where A is the aspect ratio.

Substitution of this value into Eq. (2) gives

$$C_L = 2\pi\alpha A/(EA + 2) \tag{4}$$

Since the chordwise distribution of the circulation in three-dimensional flow is assumed similar to that in two, and since the similarity is only proved for the non-circulatory flow, Eq. (4) must be considered a correction of the wing-section theory rather than a solution of the three-dimensional problem. The assumption of similarity, although its validity is subject to somewhat the same limitations in general, appears to be a more justifiable one than the assumption of equality made in the lifting-line theory.

The problem of *three-dimensional* flow around a lifting elliptical plate has been treated by Krienes[2] using

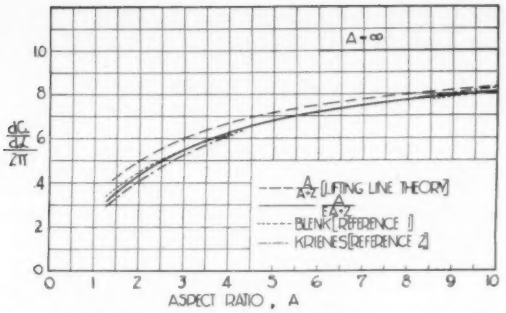

FIG. 2. Theoretical variations of lift-curve slope with aspect ratio.

Prandtl's concept of the acceleration potential. The calculations involve the superposition of a series of solutions of $\Delta^2\phi = 0$ in ellipsoidal coordinates (Lamé functions), the coefficients of the series being obtained from simultaneous equations. Although the overall lift depends on only one coefficient, calculations of the span loading and the drag would require all the terms of the infinite series and was therefore not considered practicable.

The lift coefficients obtained by Krienes' method are shown in Fig. 2. Results obtained by correcting the wing-section theory in accordance with Eq. (4) are compared with Krienes', and the agreement is seen to be good for ordinary aspect ratios.

A curve derived from Blenk's calculation of the vortex distribution in a rectangular plate[3] also agrees closely with Eq. (4).

It is found that the additional correction to the wing-section theory accounts for an appreciable fraction of the loss in lift that is usually attributed to viscosity. It has been difficult to reconcile the magnitude of the inefficiency with the observed dimensions of the wake, which in the case of smooth wings, is extremely narrow at the trailing edge. The foregoing correction accounts for as much as half of this discrepancy in cases of wings with sharp trailing edges. (See Fig. 3.)

According to Munk's theorem, the induced drag is not affected by a displacement of the lifting elements in the direction of the chord; hence the relation between the lift and the induced drag may be derived on the basis of the lifting-line theory. Also, since the pitching moment of the elliptic wing involves the same correction as the lift, no change of aerodynamic center location with aspect ratio is indicated.

The three-dimensional potential flow around the elliptic disc may be used also as the basis for calculating the lift of an elliptic wing with varying angle of attack. On account of the linearity of the equations, the general problem may be reduced to a determination of the growth of lift following a sudden start of the motion with the flight velocity V and the normal velocity $w = V\alpha$.*

* The infinite force implied by the sudden start leads, in practice, to a finite value during the continuous motions to which the formulas are applied.

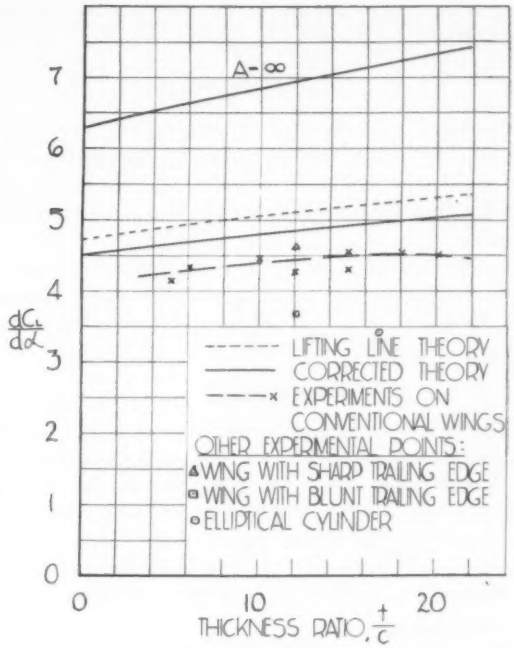

FIG. 3. Experimental and theoretical lift-curve slopes. Aspect ratio, 6.

Since the steady or asymptotic value of the lift is already known, the most important point is the determination of the lift near the start of the motion.

As a consequence of the Kutta condition, the layer of air leaving the wing at the trailing edge must satisfy the same boundary condition as the adjacent wing surface for a short distance downstream. Thus the layer of air in contact with the wing retains the motion imparted by the wing and for a short distance after the start this layer (the vortex wake) behaves as an impermeable extension of the wing surface.[4] The flow at the first instant after the start is thus what might be caused by the wing in process of growing wider at the rate V while moving with the normal velocity w. The starting lift $L_{t=0}$ may then be thought of as the reaction to uniform motion of the wing acting as a body with increasing mass:

$$L_{t=0} = w\,(dm'/dt) = w\,(dm'/dc)\,V \qquad (5)$$

where m' is the mass representing the aerodynamic inertia of the flow and c is the apparent length of the chord. In two-dimensional flow

$$m' = \pi\,(c^2/4)\rho \qquad (6)$$

so that

$$C_{L_{t=0}} = \pi\alpha \qquad (7)$$

In the case of the elliptic wing the starting process is pictured as a change into a similar but slightly wider ellipse. For normal aspect ratios this change fulfills the required conditions everywhere except near the extreme tips. The aerodynamic inertia of the elliptic

wing is the same as if the sections were in two-dimensional flow except for the factor E. Hence:

$$C_{L_{t=0}} = \pi\alpha/E$$

According to some approximate calculations (based on the lifting-line theory) made by the author,[4] the lift of the elliptic wing approaches its final value more rapidly than would be suggested by the two-dimensional theory.

In the case of $A = 3$, or in the equivalent case of $A = 6$ with the wing vibrating symmetrically in torsion, the development of lift appears to be nearly instantaneous.

Appendix

The problem of the fluid motion produced by translation of a solid ellipsoid was first solved by Green in an investigation of the vibration of pendulums. Formulas given for this problem in textbooks on hydrodynamics become indeterminate when applied to the case of an elliptic disc. The following short discussion is therefore presented to show the application to the present problem.

As explained in ref. 5, the surface potential of an ellipsoid can be given by a very simple formula. For motion along a principal axis, the potential at any point on the surface is proportional to the coordinate of the point in the direction of motion. Thus, if the ellipsoid with semiaxes $a > b > c$ along x, y, and z, respectively, is moving with unit velocity in the direction of z, the surface potential is simply

$$\phi = Cz \tag{3}$$

The equipotential lines are the similar ellipses formed by the intersection of the ellipsoidal surface with a series of equidistant parallel planes perpendicular to z. The constant C depends on the axis ratio and its evaluation involves a special class of transcendental function known as "Green's Integrals." The solution for the surface potential appears in the form:

$$\phi = [\gamma_0/(2 - \gamma_0)]z \tag{4}$$

where

$$\gamma_0 = abc \int_0^\infty \frac{d\lambda}{(c^2 + \lambda)\sqrt{(a^2 + \lambda)(b^2 + \lambda)(c^2 + \lambda)}}$$

is Green's integral.

The reduction of these integrals to the standard elliptic functions is given in ref. 5. Following equation (6.1) of ref. 5 and substituting $\lambda = 0$, in order to restrict the solution to the surface of the ellipsoid, will give

$$\gamma_0 = \frac{2abc}{\sqrt{(a^2 - c^2)^3}} \frac{a^2 - c^2}{b^2 - c^2}\left[\frac{b}{ac}\sqrt{a^2 - c^2} - E\right]$$

where E is the complete elliptic integral with the modulus $k = \sqrt{(a^2 - b^2)/a^2}$. The integral E is equal to the perimeter of a quadrant of the ellipse ab divided by the semiaxis a.[6]

$$\gamma_0 \longrightarrow 2\,[1 - (c/b)E]$$

As $c \longrightarrow 0$

Since Eq. (4) becomes indeterminate ($z \longrightarrow 0$ and $\gamma_0 \longrightarrow 2$), it is necessary to express the solution in terms of x and y, which are related to z through the equation of the ellipsoidal surface:

$$\frac{x^2}{a^2} + \frac{y^2}{b^2} + \frac{z^2}{c^2} = 1 \tag{5}$$

or

$$z = c\sqrt{1 - \frac{x^2}{a^2} - \frac{y^2}{b^2}} \tag{6}$$

Substitution for γ_0 and z in Eq. (4) gives

$$\phi = \frac{b}{E}\sqrt{1 - \frac{x^2}{a^2} - \frac{y^2}{b^2}} \tag{7}$$

or

$$(x^2/a^2) + (y^2/b^2) + [\phi^2/(b/E)^2] = 1 \tag{8}$$

Hence the distribution of the surface potential over the disc may be represented by the ordinates of a circumscribed ellipsoid having the vertical axis $2b/E$. For infinite axis ratio, $E = 1$ and the chordwise cross-sections of the potential distribution are circles of radius b.

In order to illustrate the analogy to two-dimensional flow, it is convenient to introduce the angle θ defined, at a particular value of x, by

$$\cos\theta = y/y_e \tag{9}$$

where $y_e = b\sqrt{1 - (x^2/a^2)}$ is the ordinate of the edge of the disc. Then, from Eq. (8),

$$\phi = (y_e/E)\sin\theta \tag{10}$$

which is the potential function of the two-dimensional case except for the factor $1/E$. It follows then that the edge velocity is also reduced from that in two-dimensional flow by the factor $1/E$.

References

[1] Prandtl, L., *Recent Work on Airfoil Theory*, N.A.C.A. Technical Memorandum No. 962, 1940.

[2] Krienes, Klaus, *The Elliptic Wing Based on the Potential Theory*, N.A.C.A. Technical Memorandum No. 971, 1941.

[3] von Kármán, Th., and Burgers, J. M., Vol. II, *division E of Aerodynamic Theory*, W. F. Durand, ed., Julius Springer (Berlin), 1935.

[4] Jones, Robert T., *The Unsteady Lift of a Wing of Finite Aspect Ratio*, N.A.C.A. Technical Report No. 681, 1939.

[5] Munk, Max M., *Fluid Mechanics*, Part II, Vol. I, Div. C of Aerodynamic Theory, W. F. Durand, ed., Julius Springer (Berlin), 1935, pages 293–304.

[6] Wilson, Edwin Bidwell, *Advanced Calculus*, Ginn and Co., page 514. 1912.

On Propeller-Tip Interference Due to the Proximity of a Fuselage

ALBERT GAIL* AND HO-SHEN LU†

University of Minnesota

SUMMARY

The periodic changes of the air forces acting on a propeller blade element that passes by the flanks of a fuselage nose are theoretically investigated. This forcing function known to excite vibrations of propellers and airplane structure is harmonically analyzed. The strength of the fundamental harmonic and the relative strengths of the higher harmonics are found to be greatly dependent upon the location of the propeller plane downstream from the fuselage nose and upon the ratio of fuselage diameter to propeller diameter.

The farther downstream the propeller is located behind the fuselage tip and the greater the fuselage diameter compared to the propeller diameter, the smaller is the intensity of the fundamental harmonic and the smaller is the relative importance of the higher harmonics of these propeller-tip excitations.

The clearance between propeller-tip and fuselage flank is found to have comparatively little beneficial effect within the usual limits at the designer's disposal.

The simplifying assumptions of this analysis restrict the validity of the results to fuselage shapes corresponding to a Rankine point-source half-body in flow of axial symmetry and propeller locations one fuselage diameter or more downstream from the fuselage bow.

Experimental verification of this analysis and an investigation of oblique flow about the fuselage are desirable.

INTRODUCTION

ON MULTI-ENGINE airplanes having propeller blades passing the fuselage flanks (Fig. 1) strong vibrations have been observed, the cause of which could be traced to aerodynamic interferences between propeller-tips and fuselage. These interferences are the object of this analysis.

The disturbances of the velocity field due to the presence of the fuselage change the lift and drag of the propeller blade element whenever it passes through the vicinity of the fuselage.

The absolute magnitude of the periodically changing forces acting on the blade will not be determined in this paper pending further development of the lift theory for finite wings and propellers in unsteady flow. However, the relative magnitudes of these periodically changing air forces acting on the blade are of primary concern to the designer who wants to know how to decrease these interference impulses rather than how strong they are. Moreover, he wonders how important the higher harmonics of these excitations may be since he realizes that the changes of the air forces on the blade are obviously not sinusoidally varying during each revolution of the propeller.

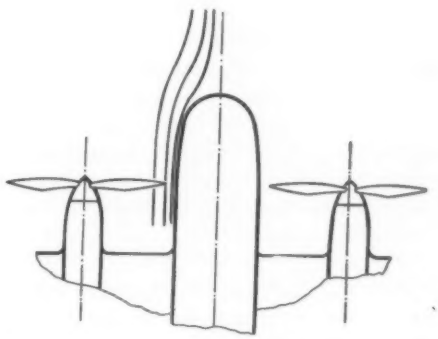

FIG. 1. The propeller-fuselage combination investigated.

This investigation is therefore concerned with the relative magnitude of the interference excitations and with the relative importance of their higher harmonics.

THE VELOCITY FIELD SURROUNDING THE FUSELAGE NOSE

The fuselage nose will be represented by a Rankine solid containing a single point source.‡ The assumptions implied in this approach are obviously: axial symmetry of flow and fuselage and a fuselage contour corresponding to that of the fluid surface separating the source flow from the superposed rectilinear flow (Fig. 5). The velocity potential of this flow is

$$\varphi = U_0 x - (Q/4\pi\sqrt{x^2 + r^2} \qquad (1)$$

where x, r = cylindrical coordinates.
X-axis = axis of symmetry with point source as origin.
Q = source intensity.
U_0 = velocity of the rectilinear superposed flow, *i.e.*, airspeed with which the airplane flies.

Expressing the source intensity Q in terms of the diameter $2\rho_0$ which the fuselage asymptotically approaches ($Q = \pi\rho_0^2 U_0$) and substituting in Eq. (1) one obtains

$$\varphi = U_0 x - (U_0\rho_0^2/4\sqrt{x^2 + r^2}) \qquad (1a)$$

Received May 17, 1941.

* Asst. Prof. Aeronautical Engineering.

† Research Fellow, Engineering Experiment Station.

‡ Lock, C. N. H. (R. & M. 1239) and Wieselsberger, C. (Z.F.M., September 28, 1932, page 533) have previously investigated the interference between a propeller and *its* nacelle employing sources and sinks.

Hence the axial or x-component of the velocity is

$$u = \frac{\partial \varphi}{\partial x} = U_0 + \frac{U_0 x \rho_0^2}{4(x^2 + r^2)^{3/2}} = U_0 + \Delta u \qquad (2)$$

where Δu is the increase of the x-component of the velocity due to the presence of the source flow (fuselage nose).

The radial component of the velocity is

$$v_r = \frac{\partial \varphi}{\partial r} = \frac{U_0 \rho_0^2 r}{4(x^2 + r^2)^{3/2}} \qquad (3)$$

v_r is so small as to be negligible for $x > \rho_0$. Moreover, the influence of v_r upon the interference impulses is not investigated here. This influence is believed to be negligible for $x > 0$. The neglecting of v_r, however, limits the scope of this analysis to locations of the propeller plane well aft of the source, *i.e.*, not farther forward than about one fuselage diameter downstream from the fuselage tip.

The Periodic Changes of Thrust and Torque Acting on a Propeller Blade Element

The change due to Δu of the flow at any blade element at a distance, a, from the propeller axis is apparent in the vector diagram Fig. 2.

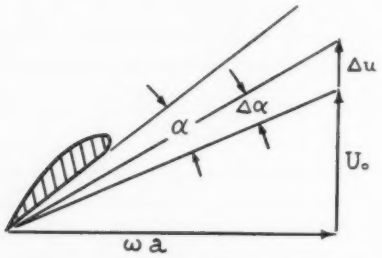

Fig. 2. The velocity vectors on a blade element.

The decrease of angle of attack due to Δu is

$$\Delta\alpha = \tan^{-1}\left[\Delta u \omega a/(U_0^2 + \Delta u U_0 + \omega^2 a^2)\right] \qquad (4)$$

or for Δu small as compared to U_0 as well as to ωa, $\Delta\alpha$ is approximately

$$\Delta\alpha = \omega a \Delta u/(U_0^2 + \omega^2 a^2) \qquad (4a)$$

Furthermore the decreases in the lift and drag of the element are proportional to $\Delta\alpha$, at least for the small values of $\Delta\alpha$ which occur in this problem. Thence the decreases in the thrust ΔT and torque ΔQ acting on the blade element will be proportional to $\Delta\alpha$ as well as to Δu

$$\begin{aligned} \Delta T &= K_1 \Delta\alpha = K_T \Delta u \\ \Delta Q &= K_2 \Delta\alpha = K_Q \Delta u \end{aligned} \qquad (5)$$

where K_1, K_2, K_T, and K_Q, are constants. These constants are influenced by propeller shape and operation conditions. They are particularly affected by the time rate of change of circulation. This analysis does not attempt to determine these constants and rather confines itself to determining the relative magnitudes of the interference excitations ΔT and ΔQ as affected by the relative dimensions of the propeller-fuselage combination.

Δu as encountered by the blade element of the propeller rotating with the angular velocity ω is obviously a function of ωt, the angular displacement of the propeller about its axis. Fig. 3 shows a front and a plan view of propeller and fuselage illustrating the dimensions involved.

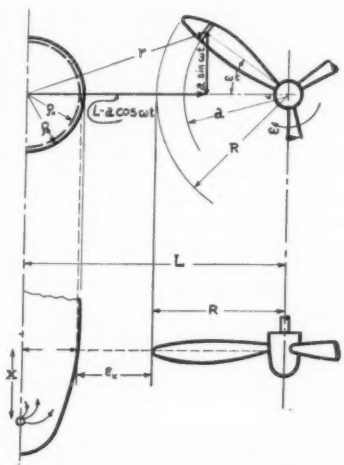

Fig. 3. Front and plan view of propeller and fuselage nose illustrating the symbols employed.

From Fig. 3 one reads:

$$\begin{aligned} r^2 &= a^2 \sin^2(\omega t) + (L - a\cos(\omega t))^2 \\ &= L^2 + a^2 - 2La\cos(\omega t) \end{aligned} \qquad (6)$$

where L = distance between X-axis and propeller axis.

$L = \epsilon_x + \rho_x + R$.

ϵ_x = propeller tip-fuselage clearance.

ρ_x = fuselage diameter in propeller plane.

R = tip radius of the propeller.

Substituting Eq. (6) in Eq. (2) one obtains Δu as a periodic function of ωt:

$$\Delta u = \frac{U_0 \rho_0^2 x}{4[x^2 + L^2 + a^2 - 2La\cos(\omega t)]^{3/2}} \qquad (7)$$

Thus the periodic changes of thrust and torque acting on the blade element

$$\begin{aligned} \Delta T &= K_T U_0 (\Delta u/U_0) \\ \Delta Q &= K_Q U_0 (\Delta u/U_0) \end{aligned} \qquad (8)$$

These periodic forces may excite vibrations of the propeller, the engine, and/or the airplane structure. Since $\Delta T = f_1(\omega t)$ and $\Delta Q = f_2(\omega t)$ are non-harmonic (Eqs. (7) and (8) and Fig. 4) a number of modes of the

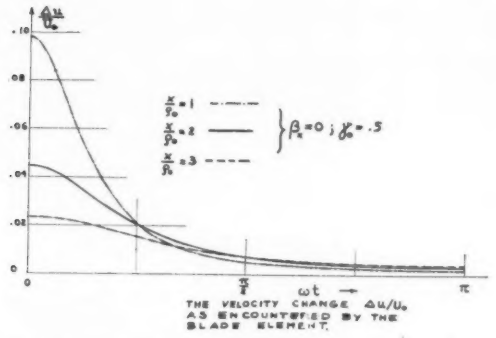

FIG. 4. The velocity change $\Delta u/U_0$ as encountered by the blade element.

responding system may be excited simultaneously. These forcing functions of the propeller-tip interference will, therefore, be subjected to a harmonic analysis.

NON-DIMENSIONAL PARAMETERS

Before entering into the Fourier expansion one may express the geometric dimensions in units of some characteristic length, say R. Thus define

$\rho_0 = \gamma_0 R =$ half the greatest fuselage diameter.
$\rho_x = \gamma_x R =$ half the local fuselage diameter at a distance x downstream from the point source.
$x = \xi R =$ location downstream from the point source.
$\epsilon_x = \beta_x R =$ propeller clearance $= L - (\rho_x + R)$.
$a = \zeta R =$ distance of the blade element from the propeller axis.

Eq. (6) may now take the dimensionless form

$$\frac{\Delta u}{U_0} = \frac{\gamma_0^2 \xi}{4}\left[\xi^2 + (1 + \beta_x + \gamma_x)^2 + \zeta^2 - 2(1 + \beta_x + \gamma_x)\zeta \cos(\omega t)\right]^{-3/2} \quad (9)$$

Let

$$A = \xi^2 + (1 + \beta_x + \gamma_x)^2 + \zeta^2$$
$$B = 2(1 + \beta_x + \gamma_x)\zeta$$
$$C = \gamma_0^2 \xi/4$$

Then Eq. (9) simplifies to

$$\Delta u/U_0 = C(A - B\cos\omega t)^{-3/2} \quad (10)$$

The fuselage radius ρ_x at any section x may be derived as follows:

Stokes stream function, ψ, for a point source in rectilinear flow is in cylindrical coordinates x and r

$$\psi = \frac{1}{2}U_0 r^2 - \frac{Q}{4\pi}\left(1 + \frac{x}{\sqrt{x^2 + r^2}}\right)$$
$$= \frac{1}{2}U_0 r^2 - \frac{1}{4}\rho_0^2 U_0\left(1 + \frac{x}{\sqrt{x^2 + r^2}}\right)$$

The fuselage corresponds to the streamline $\psi = 0$, whence, setting $r = \rho_x$ to indicate the radius of the fuselage at any x, the shape of the fuselage is given by

$$\rho_x^2 = \frac{1}{2}\rho_0^2\left(1 + \frac{x}{\sqrt{x^2 + r^2}}\right)$$

This equation may be solved for ρ_x with the result

$$\frac{\rho_x}{\rho_0} = \sqrt{\frac{1}{2}\left[1 - \left(\frac{x}{\rho_0}\right)^2 + \frac{x}{\rho_0}\sqrt{\left(\frac{x}{\rho_0}\right)^2 + 2}\right]} \quad (11)$$

The negative sign is physically meaningless as a numerical example would reveal.

The contour of the fuselage nose (Rankine point-source half-body) as determined by Eq. (11) is plotted in Fig. 5.

HARMONIC ANALYSIS OF THE PERIODIC FORCING FUNCTION

The periodic changes of thrust and torque due to the proximity of the fuselage nose are found to be functions of ωt and have the form

$$f(\omega t) = G(A - B\cos\omega t)^{-3/2} \quad (12)$$

where G, A, and B are constants for any particular airplane flying under a particular condition of operation. Eq. (12) may be transformed into

$$f(\omega t) = H(1 + \alpha^2 - 2\alpha\cos\omega t)^{-3/2} \quad (13)$$

having substituted

$$\alpha = (A/B)\left[1 - \sqrt{1 - (B/A)^2}\right] \quad (14)$$

and

$$H = G[(1 + \alpha^2)/A]^{3/2}$$

The function $(1 + \alpha^2 - 2\alpha\cos\omega t)^{-3/2}$ in which $0 < \alpha < 1$ may be expanded* into the series

$$(1 + \alpha^2 - 2\alpha\cos\omega t)^{-3/2} = b_0/2 + b_1\cos\omega t + b_2\cos 2\omega t + b_3\cos 3\omega t + \ldots\ldots + b_n\cos n\omega t = \frac{1}{2}\sum_{n=-\infty}^{n=\infty} b_n\cos n\omega t \quad (15)$$

* The authors are indebted to Dr. Isaac Opatowski for bringing to their attention the following references and to Dr. Dunham Jackson for mathematical advice.

Tisserand, F., *Traité de Mécanique Céleste*, Vol. I, pages 273–277, Gauthier Villars, Paris, 1889.

Burkhardt, H., *Trigonometrische Reihen und Integrale*, Enzyklopädie der mathematischen Wissenschaften., Vol. II, 1.

von Zeipel, H., *Entwicklung der Störungsfunktion*, Enzyklopädie der mathematischen Wissenschaften., Vol. IV, 2.

The authors will be glad to supply the mathematical details of the expansion to any reader who may be interested.

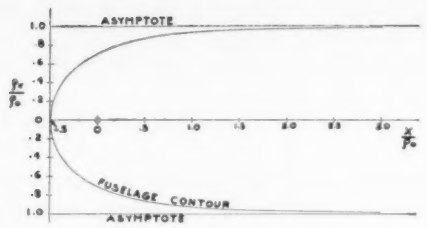

FIG. 5. The contour of a fuselage nose corresponding to a Rankine point-source half-body.

The first two coefficients b_0 and b_1 can be obtained by the following formulas.

$$b_0 = (1 - \alpha^2)^{-2}\left[(1 + \alpha^2)\frac{4}{\pi}F\left(\alpha, \frac{\pi}{2}\right) - \frac{8}{\pi}\left\{F\left(\alpha, \frac{\pi}{2}\right) - E\left(\alpha, \frac{\pi}{2}\right)\right\}\right] \quad (16)$$

$$b_1 = (1 - \alpha^2)^{-2}\left[\frac{8\alpha}{\pi}F\left(\alpha, \frac{\pi}{2}\right) - (1 + \alpha^2)\frac{4}{\pi\alpha}\left\{F\left(\alpha, \frac{\pi}{2}\right) - E\left(\alpha, \frac{\pi}{2}\right)\right\}\right] \quad (17)$$

where

$$F\left(\alpha, \frac{\pi}{2}\right) = \int_0^{\pi/2} \frac{d(\omega t)}{\sqrt{1 - \alpha^2 \sin^2(\omega t)}} =$$

complete elliptic integral of the first kind.

$$E\left(\alpha, \frac{\pi}{2}\right) = \int_0^{\pi/2} \sqrt{1 - \alpha^2 \sin^2(\omega t)}\, d(\omega t) =$$

complete elliptic integral of the second kind.

For $0 < \alpha < 1$ the higher harmonics are

$$b_2 = 2\left(\alpha + \frac{1}{\alpha}\right)b_1 - 3b_0$$

$$b_3 = \frac{4}{3}\left(\alpha + \frac{1}{\alpha}\right)b_2 - \frac{5}{3}b_1 \quad (18)$$

$$b_4 = \frac{6}{5}\left(\alpha + \frac{1}{\alpha}\right)b_3 - \frac{7}{5}b_2$$

or

$$b_{n+1} = \frac{2n}{2n-1}\left(\alpha + \frac{1}{\alpha}\right)b_n - \frac{2n+1}{2n-1}b_{n-1}$$

Eq. (18) determines the coefficient of any higher harmonic term when the coefficient of the previous two successive harmonics is known.

The coefficients b_1 have been calculated for $0 < \alpha < 1$ and are plotted in Fig. 6.

The coefficients of the higher harmonics were determined by means of Eq. (18) and are expressed as multiples of b_1 in Fig. 7.

Although Eq. (15) and thence $b_1, b_2, \ldots\ldots b_n$ do not express the complete forcing function it becomes clear from Figs. 6 and 7 that α is a major parameter determining the magnitude of the fundamental and the relative strength of the higher harmonics.

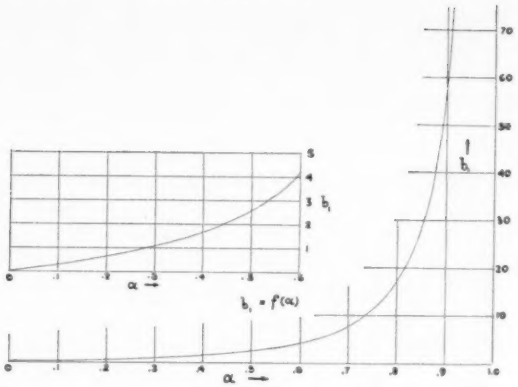

FIG. 6. $b_1 = f(\alpha)$.

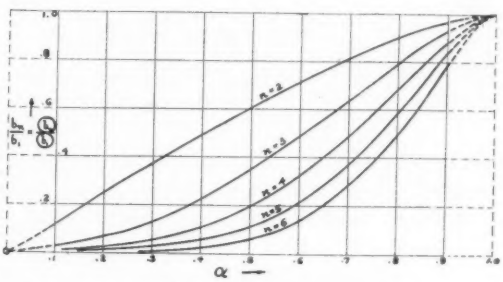

FIG. 7. $b_n/b_1 = f(\alpha)$. (Circled notations refer to $\mathbf{b}_n$ and $\mathbf{b}_1$ as used in text.)

α itself depends upon the geometric dimensions of the propeller—fuselage combination, *i.e.*, γ_0, x/ρ_0, ζ, β_x. (Eq. (14).)

Fig. 8 shows α in a three-dimensional diagram as a function of γ_0, the diameter ratio of fuselage and propeller, and x/ρ_0, the aft location of the propeller plane

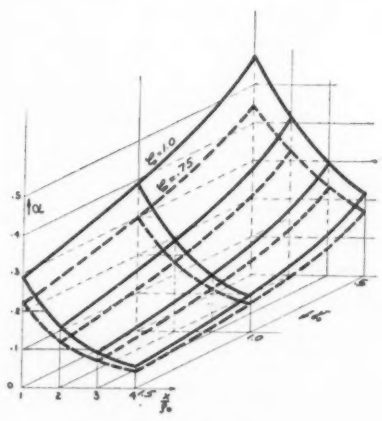

FIG. 8.

downstream from the point source. It is noteworthy that the aft location x/ρ_0 of the propeller plane and the diameter ratio of the fuselage and propeller have the greatest effect on α (Fig. 8) and on the magnitude of the harmonics (Figs. 6 and 7). The location of the propeller section, $\zeta = a/R$, has a comparatively lesser influence. This holds true for the same reason for the propeller-tip clearance.

It must be remembered that Eq. (15) is not the complete forcing function. Expanding ΔT and ΔQ in a Fourier series

$$\Delta T = K_T U_0 \frac{\gamma_0 \xi}{4}\left(\frac{1+\alpha^2}{A}\right)^{3/2}\left(\frac{b_0}{2} + b_1 \cos \omega t + b_2 \cos 2\omega t + \ldots\ldots\right) \tag{19}$$

$$\Delta Q = K_Q U_0 \frac{\gamma_0 \xi}{4}\left(\frac{1+\alpha^2}{A}\right)^{3/2}\left(\frac{b_0}{2} + b_1 \cos \omega t + \ldots\ldots\right)$$

defining

$$\mathbf{b}_n = \frac{\gamma_0 \xi}{4}\left[\frac{1+\alpha^2}{A}\right]^{3/2} b_n$$

$$\Delta T = K_T U_0[(\mathbf{b}_0/2) + \mathbf{b}_1 \cos \omega t + \mathbf{b}_2 \cos 2\omega t + \mathbf{b}_3 \cos 3\omega t + \ldots\ldots] \tag{20}$$

$$\Delta Q = K_Q U_0[(\mathbf{b}_0/2) + \mathbf{b}_1 \cos \omega t + \ldots\ldots]$$

Thus the coefficient $\mathbf{b}_1$ is a measure of the strength of the first harmonic of the tip interference excitations so long as the operation conditions, *i.e.*, U_0, r.p.m. and propeller pitch, are kept constant. Under the same conditions $\mathbf{b}_n/\mathbf{b}_1$ is a measure of the relative strength of the higher harmonics of these excitations.

Fig. 9 shows $\mathbf{b}_1$ *vs.* x/ρ_0 and γ_0 for the propeller-tip section ($\zeta = 1.0$) and the $0.75R$ station ($\zeta = 0.75$).

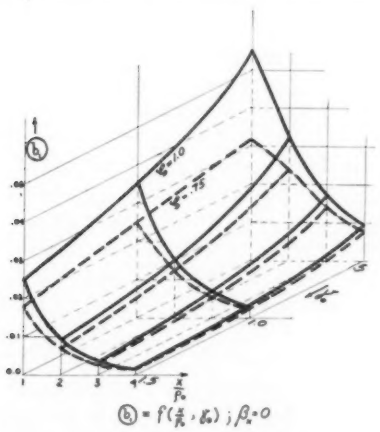

FIG. 9. (The circled notation b_1 refers to $\mathbf{b}_1$ as used in text.)

$\mathbf{b}_n/\mathbf{b}_1$ is shown in Fig. 7 as a function of α which in turn depends on x/ρ_0, γ_0, ζ and β_x as shown in Fig. 8.

RESULTS AND CONCLUSIONS

The periodic changes of thrust, ΔT, and torque, ΔQ, acting on a blade element which passes by the flank of a fuselage nose are expressed as functions of the velocity increase Δu due to the proximity of the fuselage (Eq. (8)). The relative velocity increase $\Delta u/U_0$ is a periodic function of the angle of blade rotation ωt (Eqs. (9) and (10) and Fig. 4) and also depends on the relative dimensions of the propeller-fuselage combination.

The periodic functions, ΔT and ΔQ, are then expanded into Fourier series (Eq. (20)) the coefficients of which, $\mathbf{b}_n$, are found to depend upon the relative dimensions of the propeller-fuselage combination, *i.e.*, γ_0, x/ρ_0, ζ, (β_x) as shown in Figs. 7, 8, and 9.

These figures indicate the following practical results:

(1) The relative dimensions of the propeller-fuselage combination affect the strength of the fundamental harmonic $\mathbf{b}_1$ as well as the relative strengths of the higher harmonics $\mathbf{b}_n/\mathbf{b}_1$ in the same sense.

(2) The greater the fuselage diameter as compared to the propeller diameter, *i.e.*, the greater $\rho_0/R = \gamma_0$ the smaller are $\mathbf{b}_1$ and $\mathbf{b}_n/\mathbf{b}_1$. This result is valid only if one compares the excitations of propellers having the same diameters, blade angle, blade shape, and r.p.m. in combination with fuselages of various diameters. The interference excitations can obviously not continue to increase as the fuselage diameter decreases to zero; they do, however, increase for γ_0 between 0.5 and 1.5 within which limits conventional airplanes are believed to stay. The diameters of fuselage and propeller are determined by the designer on the basis of more important considerations than the propeller-tip excitations. It would also be out of the question to change either one of these diameters in order to remedy intolerable vibrations due to these interferences. γ_0 must therefore be considered an unchangeable constant for a given airplane.

(3) As might have been expected, the intensity of the interference excitations diminishes the farther away from the fuselage the blade element passes. Hence, the blade tip sections ($\zeta = 1.0$) experience stronger excitations than for instance those at $0.75R$ ($\zeta = 0.75$). Likewise beneficial decreases result from increased clearances between propeller tips and fuselage flank, $\beta_x = \epsilon_x/R$. The effects of changes of the propeller clearance are disappointingly small considering that the clearance can usually be changed by a few inches at the most, which is a very small fraction of the propeller radius. Practically no remedy can be expected for undesirable vibrations due to these tip interferences by increases of the propeller-tip clearance within such limits.

The variation of the interference forces along the blade (ΔT and $\Delta Q = f(\zeta)$) is of interest for the analysis of vibrations of the propeller blades.

(4) The intensity of the interference excitations $\mathbf{b}_1$ and $\mathbf{b}_n/\mathbf{b}_1$ is greatly dependent upon how far aft (downstream) of the fuselage tip the propeller plane is located. The farther aft of the fuselage tip the propeller plane is located, *i.e.*, the greater x/ρ_0, the less intense are the

interference excitations. This statement holds only for values of $x/\rho_0 > 1$, *i.e.*, for propellers about one or more fuselage diameters aft of the fuselage tip. In the immediate vicinity of the fuselage tip, *i.e.*, $-1 < x/\rho_0 < +1$, the assumptions of the derivation of the forcing function ($v_r = 0$) do not hold.

It is of interest to the designer that fuselages protruding far ahead between the propellers produce much smaller propeller-tip interference impulses than fuselages that extend only about one fuselage diameter ahead of the propeller plane. This may not be a sufficient reason to decide the extent by which the fuselage nose is to protrude. This point of view, however, deserves consideration as an argument in favor of a far-protruding fuselage nose.

The influence of the relative locations of fuselage tip and propeller plane, x/ρ_0, upon the intensity of the interferences is here determined for one particular fuselage contour only (Fig. 5). It must be expected that differently shaped fuselages would behave differently in this respect, because the origin of the interference is the velocity change Δu as encountered by the blade element and as produced by the presence of the fuselage. The rate of change of Δu in the direction normal to the fuselage surface obviously affects the sharpness of the increase and decrease of ΔT and $\Delta Q = f(\omega t)$; the rate of change of Δu must be the greater the smaller the radius of curvature of the fuselage contour ($\rho_x = f(x)$). This must be so since the greater centrifugal forces on sharply curved streamlines call for equally greater centripetal pressure gradients which in turn are accompanied by rapid decreases of velocity normal to the streamlines in accordance with Bernoulli's equation.

In the light of this interpretation the decrease in intensity of the interference impulses for increasing values of x/ρ_0 is largely due to the decrease of curvature (increase of radius of curvature) of the fuselage contour downstream from the fuselage tip. This leads to the speculation that a locally restricted deformation of the fuselage flanks where the propeller tips pass by may control the inflow disturbances Δu in such a manner as to decrease the interference excitations materially. An experimental investigation of the effectiveness of such a simple remedy would be most desirable.

Furthermore, this analysis must be amplified by an investigation of oblique flow about the fuselage which is ever present on account of the induced velocity of the bound vortex of the wing and the inclination of the fuselage itself in many flight conditions. Such an investigation is believed to yield to theoretical treatment along the lines of von Kármán's analysis of the flow pattern around airships in oblique flow. (Ref.: von Kármán, N.A.C.A. Technical Memorandum No. 574, *Calculation of Pressure Distribution on Airship Hulls*.)

Finally, it may be mentioned that the results of this paper are also applicable to the analogous interferences of ships' propellers.

An Approximate Method to Predict the Transition or "Flare" Flight Path in the Take-off or Landing of an Airplane

OMER WELLING*

Civil Aeronautics Administration

SUMMARY

The nature of the transition phase of the take-off and landing of an airplane is briefly discussed in which it is shown that, in the usual case, the two maneuvers are virtually identical physically, since in each the airplane may be considered to be a free body being simultaneously accelerated by two mutually perpendicular forces between similar end conditions. It is also shown that the time histories of the two accelerating forces are in each case so interrelated that one determines the other and that therefore the pilot may control the time history of one of the forces directly, in which case that for the other is automatically determined; or he may indirectly control the time history of the other force through his direct control of the one, in which case the necessary time history for the directly controlled force is automatically determined; but he cannot exercise independent control over both forces in any case.

Typical time histories of these forces have been obtained for one airplane in take-off and for two airplanes in landing by means of step-by-step integration of the summation force equations which may be written. From these solutions it appears that the possible time histories which will satisfy a given set of end conditions lie within fairly narrow limits. Based upon a simple geometrical approximation to the form of these typical time histories, a method is presented by means of which to predict the flight path in terms of the initial and final values of flight path and climbing or sinking speeds and of the thrust and/or drag characteristics of the airplane.

INTRODUCTION

THE problem of establishing the dimensions of the minimum size airport into or out of which an airplane may safely be operated has received considerable attention in the air transport industry during recent years. This has proved to be a complex and difficult problem involving the performance of the airplane, the behavior of the pilot, the geographical and meteorological conditions at and surrounding the airport site, and other related factors. The basic item of performance involved in the problem is the flight path described by the airplane during the process of taking off and landing.

The complete take-off of an airplane may be considered to take place in three phases, *viz.:* the ground run, during which the airplane is accelerated horizontally from a standing start to a take-off or "unstick" speed at the point of leaving the ground; the transition from level flight, at the instant of "unstick," to steady climbing flight during which the airplane is accelerated upward from zero rate of climb to the rate which exists at the climbing flight path speed chosen and is also accelerated along the flight path from the "unstick" speed to the climbing speed; and finally, steady climbing flight during which the airplane is assumed to move with uniform rectilinear motion along a flight path making an angle with the horizontal.

Similarly, the complete landing may be considered to involve the following three phases: the approach glide which may be assumed to be a steady condition consisting of uniform rectilinear motion along a flight path making an angle with the horizontal; the transition from steady gliding flight to substantially level flight at the point of contact, during which the airplane is accelerated upward from the rate of descent in the approach glide to substantially zero at contact and is also decelerated along the flight path from the flight path speed during the approach glide to substantially the stalling speed at contact; and finally, the ground run during which the airplane is accelerated horizontally from the contact speed to zero.

All of the phases identified above, except the transitions, have in the past received sufficient attention that fairly generally accepted methods exist by means of which to calculate the dimensions involved in each. Such is, however, not the case for the transitions, the problem of predicting the flight paths for which is considered here.

DISCUSSION

The following discussion of the nature of these transitions is divided into a separate discussion of that which occurs during take-off and that during landing because, although the two may be considered to be dynamically similar (each involving substantially simultaneous accelerations in two mutually perpendicular directions), one is chronologically the reverse process of the other and the pilot technique involved in each is believed to be fundamentally different.

There follows a list of symbols which are used:

A = a constant
B = a constant
C = rate of climb (ft. per sec.), positive upward; coefficient
D = drag (lbs.)
E = energy (lb., ft.)
F = force (lbs.), positive upward and flightwise
G = velocity with respect to and parallel to the ground (ft. per sec.), positive flightwise

Received July 26, 1941.

* Chief, Flight Analysis Section, Flight Engineering and Factory Inspection Division.

L = lift (lbs.); (subscript)—lift
N = an exponent
S = distance parallel to the ground (ft.)
T = thrust (lbs.)
V = airspeed (ft. per sec.), positive flightwise
W = gross weight
a = acceleration (ft. per sec.^{2})
c (subscript)—climb, contact
e (subscript)—effective
g = acceleration of gravity = 32.2 ft. per sec.^{2}; (subscript)—glide
h = height (ft.), positive if measured upward; (subscript)—horizontal; *i.e.*, along the flight path
k (subscript)—kinetic
l (subscript)—landing
o (subscript)—initial
p (subscript)—potential
t = time (sec.)
v (subscript)—vertical
w (subscript)—wind
β = flight path angle (radians) = C/G

Take-off

The take-off transition or "flare" may be executed in several ways. The airplane may be gradually accelerated upward from "unstick" until steady climb is established at the chosen climbing airspeed or the pilot may allow the airplane to continue to accelerate along the flight path without gaining height until some speed in excess of the "unstick" speed is attained before beginning the upward acceleration which produces climb. This initial speed in excess of "unstick" may be less than the climbing speed or greater, in which latter case the early stage of the transition is a "zoom." There is reason to believe, however, that for a given set of end conditions the differences in the overall distances required due to possible differences in the intervening execution are negligible for all practical purposes. It also appears from an examination of a great number of photographic records of take-off flight paths that in the typical case the initial flight path speed is less than the climbing speed and the climb is continuously accelerated from zero at the beginning to that which results from a chosen climbing speed and throttle setting. The pilot technique required for a given throttle setting is so to manipulate the elevator control that the climbing airspeed is attained but not exceeded.

The flight path for such a typical transition may be represented by the diagram in Fig. 1, which also illustrates the forces acting upon the airplane. Since in the usual case β_c is of the order 10° or less it is assumed that $\sin\beta = \beta$ and $\cos\beta = 1.00$ and the following summation equations may be written with respect to the flight path:

At the beginning of the transition:

$$\begin{aligned} G &= G_o = V_o \mp V_w \\ C &= 0 \\ \Sigma_v &= L - W = 0 \\ \Sigma_h &= T - D = F_h \end{aligned}$$

At any point during the transition:

$$\begin{aligned} G &= G = V \mp V_w \\ C &= C \\ \Sigma_v &= L - W = F_v \\ \Sigma_h &= T - D - \beta W = F_h \end{aligned}$$

At the end of the transition:

$$\begin{aligned} G &= G_c = V_c \mp V_w \\ C &= C_c \\ \Sigma_v &= L - W = 0 \\ \Sigma_h &= T - D - \beta_c W = 0 \end{aligned}$$

A study of the above equations leads to the following conclusions:

(a) The pilot's control of flight path speed is largely indirect since the immediate response of the airplane to elevator control is a change in angle of attack which directly affects F_v but, aside from the comparatively negligible possible change in D, affects F_h only through the change in the βW term in the Σ_h equation due to the change in C produced by F_v.

(b) It follows that in order that the flight path speed be continuously accelerated from V_o to V_c, it is necessary that the climb be accelerated continuously from 0 to C_c and at such rate as to produce the desired flight path accelerations.

(c) It follows further that F_v must increase from zero initially to some finite value and return to zero at the end of the maneuver, while in the same time and as a result thereof, F_h must be reduced from $T - D$ initially to zero at V_c.

(d) A formal solution of the equations for the purpose of predicting the flight path appears, if not impossible, then at least likely to be so involved as to be of no practical value.

A solution to these equations has been obtained by means of step-by-step integration for a typical air carrier airplane for a transition assumed to take place between 1.15 V_s and 1.33 V_s, which was subsequently checked by photographic records of flight tests in which good agreement was obtained. This solution required a running assumption of C_L, the correctness of which assumption could be judged only after the solu-

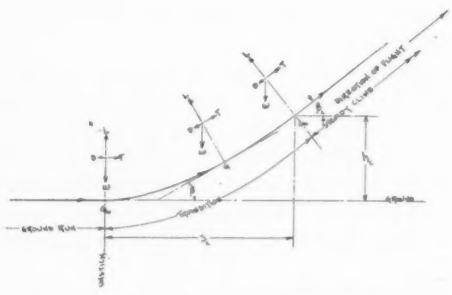

Fig. 1. Typical take-off transition flight path. (Vertical scale is of the order 5 times the horizontal.)

tion had proceeded far enough to make it apparent that the end conditions would or would not be satisfied. Experience with this solution indicated that the time history of F_v which would satisfy the end conditions lay within a comparatively narrow band of values at any time, although no difficulty in executing the maneuver was experienced by the pilot. It follows from conclusions (a), (b) and (c) above that F_h must be equally narrowly defined. Typical time histories of these two forces are shown in Fig. 2. The flight path approximates quite closely to a parabola.

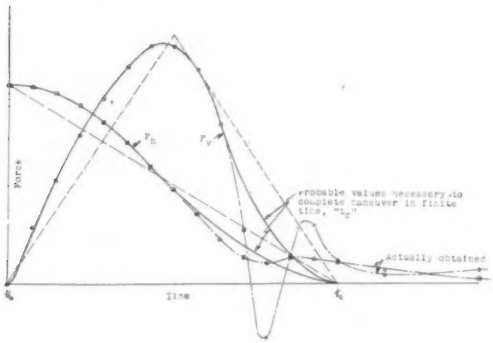

FIG. 2. Typical time histories of F_v and F_h during the take-off "Flare."

LANDING

There appears to be somewhat less likelihood of appreciable variation in the manner of executing the landing "flare" than is possible in the case of take-off primarily because the freedom of choice on the part of the pilot is almost entirely limited to the selection of the conditions from which it is begun. He may select the steady gliding speed, the rate of descent (if power is used), and the height above ground at which to begin the transition. Once these three selections have been made, however, the pilot has little choice but to reduce the sinking speed to zero at the ground, interrupt the maneuver, or "crack up." For reasons analogous to those discussed under "Take-off," the time history of F_v which will accomplish this is fairly narrowly defined and there will accompany this deceleration of the sinking speed an uncontrolled but necessary deceleration of the flight path speed.

The critical consideration in the selection of the initial conditions is to insure that this deceleration of the flight path speed does not reduce the speed to the stalling speed before reaching the ground. For this reason the maneuver is ordinarily deliberately so executed as to arrive at the ground at a flight path airspeed in excess of the stalling speed. The airplane may then be set onto the ground immediately or allowed to float just off it until the stalling speed is reached when it will settle on.

A typical landing transition flight path is illustrated by Fig. 3, which also shows the forces acting upon the

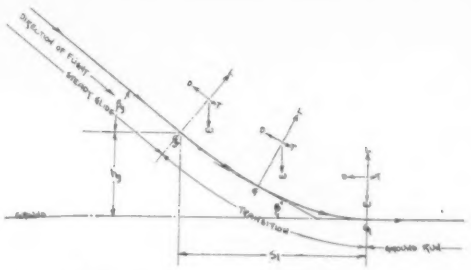

FIG. 3. Typical landing transition flight path. (Vertical scale is of the order 5 times the horizontal.)

airplane. Making the same assumptions as in the case of take-off, these equations may be written with respect to the flight path:

At the beginning of the transition:

$$\begin{aligned} G &= G_g = V_g \mp V_w \\ C &= C_g \\ \Sigma_v &= L - W = 0 \\ \Sigma_h &= T - D - \beta_g W \end{aligned}$$

At any point in the transition:

$$\begin{aligned} G &= G \\ C &\doteq C \\ \Sigma_v &= L - W = F_v \\ \Sigma_h &= T - D - \beta W = F_h \end{aligned}$$

At the end of the transition:

$$\begin{aligned} G &= G_l \\ C &= 0 \\ \Sigma_v &= L - W = 0 \\ \Sigma_h &= T - D = F_h \end{aligned}$$

These equations are identical with those written for the take-off transition and indicate a relation between F_v and F_h of the same nature as that in take-off. They also appear equally difficult of formal solution. A solution of the equations has been obtained by means of step-by-step integration for the air carrier airplane investigated under take-off and also for a typical light airplane. These transitions took place between 1.18 and 1.06 V_s and zero thrust was assumed. The time histories of F_v and F_h obtained by this means have been plotted non-dimensionally in Fig. 4 in such fashion as to indicate the relative magnitudes of these forces for each case. It should be noted that the form of each of these curves for each case is practically identical. The flight path for each case also approximates closely to a parabola.

APPROXIMATE METHOD TO PREDICT FLIGHT PATH

The following approximate solution rests upon the assumption that the actual time histories of F_v and F_h can be adequately represented by the nearest triangle of the same approximate form and enclosing the same area. These assumed equivalent histories are indi-

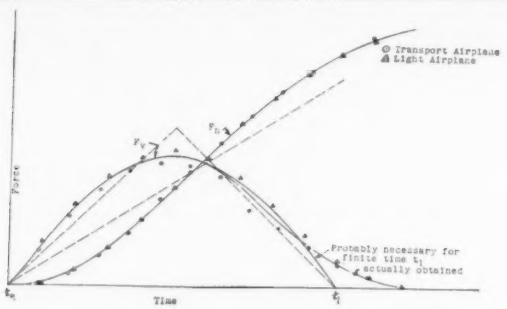

FIG. 4. Typical time histories of F_v and F_h during the landing "Flare."

cated by the dotted lines in Figs. 2 and 4. The solution consists of the following three steps:

(a) The establishment of a relation between h_c and S_c (see Figs. 1 and 3) in terms of C_c and the initial and final values of G.

(b) Derivation of the equation for the parabola to which the flight path approximates.

(c) The development of equations by means of which to calculate h and S from the thrust and drag characteristics of the airplane.

The complete solution is presented for take-off but is indicated only for landing in the interests of brevity.

TAKE-OFF (SEE FIG. 1)

1. h_c/S_c

Assume these effective constant forces:

$$F_{e_v} \text{ producing } \Delta C = C_c - 0, \text{ in } t_c$$

$$F_{e_h} \text{ producing } \Delta G = G_c - G_o, \text{ in } t_c$$

Then:

$$\Delta C = C_c = (F_{e_v} g/W)t_c, \text{ or: } F_{e_v} = C_c W/gt_c$$

and:

$$\Delta G = G_c - G_o = (F_{e_h} g/W)t_c, \text{ or: } F_{e_h} = W(G_c - G_o)/gt_c$$

Therefore:

$$F_{e_v}/F_{e_h} = C_c/(G_c - G_o) \qquad \text{(a)}$$

If the actual forces were in fact constant, the following relations would exist:

$$h_c = \overline{\Delta C}^2/2a_{e_v} = WC_c^2/2gF_{e_v}, \text{ since } a = F/M = F_e/W$$

$$S_c = G_o t_c + (\overline{\Delta G}^2/2a_{e_h} = G_o t_c + [W(G_c - G_o)^2/2gF_{e_h}]$$

Now:

$$t_c = S_c/\left(G_o + \frac{\Delta G}{2}\right) = S_c/\left(G_o + \frac{G_c}{2} - \frac{G_o}{2}\right) = 2S_c/(G_o + G_c)$$

Therefore:

$$S_c \times \left[1 - \frac{2G_o}{G_o + G_c}\right] = \frac{W(G_c - G_o)^2}{2gF_{e_h}}$$

$$S_c = \frac{W(G_c - G_o)^2}{2gF_{e_h}} \times \frac{G_o + G_c}{G_c - G_o} = \frac{W(G_c^2 - G_o^2)}{2gF_{e_h}}$$

Then:

$$h_c/S_c = \frac{WC_c^2}{2gF_{e_v}} \times \frac{2gF_{e_h}}{W(G_c^2 - G_o^2)} = \frac{C_c^2 F_{e_h}}{(G_c^2 - G_o^2)F_{e_v}}$$

But:

$$F_{e_v}/F_{e_h} = C_c/(G_c - G_o)$$

Therefore:

$$h_c/S_c = \frac{C_c^2}{G_c^2 - G_o^2} \times \frac{G_c - G_o}{C_c} = \frac{C_c}{G_c + G_o} \qquad \text{(b)}$$

Also:

$$h_c = (a_{e_v} t_c^2/2) = F_{e_v} g t_c^2/2W$$

and:

$$S_c = G_o t_c + (a_{e_h} t_c^2/2) = G_o t_c + (F_{e_h} t_c^2/2W)$$

The equivalent relation to (b) above will now be established for the assumed actual forces. Referring to Fig. 2, it may be seen that these latter forces may be expressed in terms of the effective forces thus:

$$F_v = (4F_{e_v} t/t_c)t \qquad (t = 0 \text{ to } t = t_c/2)$$

$$= 4F_{e_v} - (4F_{e_v}/t_c)t \qquad (t = t_c/2 \text{ to } t = t_c)$$

and:

$$F_h = 2F_{e_h} - (2F_{e_h}/t_c)t \qquad (t = 0 \text{ to } = t_c)$$

Then:

$$C = \int a dt = g/w \int F_t dt$$

$$= g/W \int \frac{4F_{e_v}}{t_c} t dt = \frac{2gF_{e_v}}{Wt_c} t^2 + \text{a constant} \quad (t = 0 \text{ to } t = t_c/2)$$

or, since $C = 0$ when $t = 0$, the constant $= 0$, and

$$C = (2gF_{e_v}/Wt_c)t^2 \quad (t = 0 \text{ to } t = t_c/2)$$

$$= g/W \int 4F_{e_v} - \frac{4F_{e_v}}{t_c} t dt = \frac{4gF_{e_v}}{W} t - \frac{2gF_{e_v}}{Wt_c} t^2 + \text{a constant} \quad (t = t_c/2 \text{ to } t = t_c)$$

Now:

$$C = (gF_{e_v}/2W)t_c \text{ when } t = t_c/2$$

Therefore the constant $=$

$$(gF_{e_v}/2W)t_c + (gF_{e_v}/2W)t_c - (2gF_{e_v}/W)t_c = -(gF_{e_v}/W)t_c,$$

and:

$$C = (gF_{e_v}/W)\ [4t - 2(t^2/t_c) - t_c] \quad (t = t_c/2 \text{ to } t = t_c)$$

Also:

$$G = \int a_h dt = g/W \int F_h dt = (2gF_{e_h}/W) \int 1 - (t/t_c)dt$$

$$= (2gF_{e_h}/W)[t - (t^2/2t_c)] + G_o \ (t = 0 \text{ to } t = t_c)$$

and:

$$h_c = \int_0^{t_c} Cdt = (gF_{e_v}/W)\left[\int_0^{t_c/2} (2/t_c)\ t^2 dt + \int_{t_c/2}^{t_c} 4t - 2(t^2/t_c) - t_c dt\right]$$

$$= (gF_{e_v}/W)\left\{\left[(2/3t_c)t^3 + \text{a constant}\right]_0^{t_c/2} + \left[2t^2 - (2/3t_c)t^3 - t_c t + \text{a constant}\right]_{t_c/2}^{t_c}\right\}$$

The first constant = 0 since when $t = 0$, $h_c = 0$. When $t = t_c/2$, however,

$$h_c = (gF_{e_v}/W)(2t^3/3t_c)_{t=t_c/2}$$

$$= (gF_{e_v}/W)(t_c^2/12)$$

Therefore the second constant =

$$(t_c^2/12) - (t_c^2/2) + (t_c^2/12) + (t_c^2/2) = (t_c^2/6)$$

and:

$$h_c = \frac{gF_{e_v}}{W}\left\{\left[\frac{2}{3t_c}t^3\right]_0^{t_c/2} + \left[2t^2 - \frac{2}{3t_c}t^3 - t_c + \frac{t_c^2}{6}\right]_{t_c/2}^{t_c}\right\}$$

$$= \frac{gF_{e_v}}{W}\left(\frac{t_c^2}{12} + 2t_c^2 - \frac{2}{3}t_c^2 - t_c^2 + \frac{t_c^2}{6} - \frac{t_c^2}{2} + \frac{t_c^2}{12} + \frac{t_c^2}{2} - \frac{t_c^2}{6}\right)$$

$$h_c = gF_{e_v}t_c^2/2W$$

while:

$$S_c = \int_0^{t_c} Gdt = \int_0^{t_c} G_o + (2gF_{e_h}/W)[t - (1/2t_c)t^2]dt$$

$$= G_o t_c + (2gF_{e_h}/W)[(t_c^2/2) - (t_c^2/6) + \text{a constant}]$$

Since $S = 0$ when $t = 0$, the constant = 0

and:

$$S_c = G_o t_c + (2gF_{e_h}/3W)t_c^2$$

A comparison of these expressions for h_c and S_c with those obtained above when F_e is assumed constant will show that the two expressions for h_c are identical while those for S_c differ in that the second term under the assumed actual conditions is $^2/_3 \div {}^1/_2 = {}^4/_3$ of that when F_{e_h} is assumed constant. It follows that, for the assumed actual conditions:

$$h_c = WC_c^2/2gF_{e_v}$$

and:

$$S_c = G_o t_c + {}^4/_3 \times \frac{W(G_c - G_o)^2}{2gF_{e_h}} = G_o t_c + \frac{2W(G_c - G_o)^2}{3gF_{e_h}}$$

It also follows that the average value of ΔG is $^4/_3$ of that when F_{e_h} is assumed constant, *i.e.*:

$$t_c = \frac{S_c}{G_o + {}^4/_3 \times \frac{\Delta G}{2}} = \frac{S_c}{G_o + \frac{2G_c}{3} - \frac{2G_c}{3}} = \frac{3S_c}{G_o + 2G_c}$$

Substituting this value into the expression for S_c:

$$S_c = \frac{3G_o}{G_o + 2G_c} S_c + \frac{2W(G_c - G_o)^2}{3gF_{e_h}}$$

Then:

$$S_c\left(1 - \frac{3G_o}{G_o + 2G_c}\right) = \frac{2W(G_c - G_o)^2}{3gF_{e_h}} = \left(\frac{G_o + 2G_c - 3G_o}{G_o + 2G_c}\right) S_c$$

$$S_c = \frac{2W(G_c - G_o)^2}{3gF_{e_h}} \times \frac{G_o + 2G_c}{2(G_c - G_o)} = \frac{W(G_c - G_o)(G_o + 2G_c)}{3gF_{e_h}}$$

$$h_c/S_c = \frac{WC_c^2}{2gF_{e_v}} \times \frac{3gF_{e_h}}{2W(G_c - G_o)(G_o + 2G_c)F_{e_v}} = \frac{3C_c^2 F_{e_h}}{2(G_c - G_o)(G_o + 2G_c)F_{e_v}}$$

But:

$$F_{e_v}/F_{e_h} = C_c/(G_c - G_o)$$

Therefore:

$$h_c/S_c = \frac{3C_c^2(G_c - G_o)}{2C_c(G_c - G_o)(G_o + 2G_c)} = \frac{1.5C_c}{G_o + 2G_c} \quad (1)$$

2. $h = AS^N$ (see Fig. 1)

Assume:

$$h = AS^N$$

Then:

$$dh/ds = NAS^{N-1}$$

Now:

when $S = S_c$, $h = h_c$ and $dh/ds = \beta_c = C_c/G_c$ *i.e.*:

$$NAS_c^{N-1} = C_c/G_c$$

whence:

$$A = C_c/G_c N S_c^{N-1}$$

Substituting back into the original equation:

$$h_c = C_c S_c^N / G_c N S_c^{N-1} = C_c S_c / G_c N$$

or:

$N = C_c S_c / G_c h_c$, or, since $h_c/S_c = 1.5C_c/(G_o + 2G_c)$

$N = (C_c/G_c) \times [(G_o + 2G_c)/1.5G_c] = (G_o + 2G_c)/1.5G_c$

and:

$$h/h_c = (S/S_c)^{\frac{G_o + 2G_c}{1.5G_c}} \qquad (2)$$

3. Dimensions (see Fig. 1)

At the beginning of the transition the total energy with respect to the ground is the kinetic energy of the motion, *i.e.*:

$$E_o = MG_o^2/2$$

At the end of the transition the total energy is made up of a kinetic and a potential portion, thus:

$$E_c = (MG_c^2/2) + Wh_c$$

The total energy change is, therefore:

$$\Delta E = E_c - E_o = W\left[\frac{G_c^2 - G_o^2}{2g} + h_c\right]$$

It is apparent that this change in energy has been produced by the effective value of the total accelerating force, $(T - D)_e$ acting through the distance traveled by the airplane along its flight path. Consistently with the assumption that $\cos \beta = 1.00$, this distance along the flight path is assumed equal to S_c. It follows that:

$$(T - D)_e S_c = W\left[\frac{G_c^2 - G_o^2}{2g} + h_c\right]$$

or:

$$S_c = \frac{W}{(T - D)_e}\left[\frac{G_c^2 - G_o^2}{2g} + h_c\right]$$

But:

$h_c = [1.5C_c/(G_o + 2G_c)]S_c$, from Eq. (1)

Therefore:

$$(T - D)_e S_c = (W(G_c^2 - G_o^2)/2g) + [1.5WC_c/(G_o + 2G_c)]S_c$$

$$\left[(T - D)_e - \frac{1.5WC_c}{G_o + 2G_c}\right] S_c = W(G_c^2 - G_o^2)/2g$$

$$\left[\frac{(T - D)_e(G_o + 2G_c) - 1.5C_cW}{G_o + 2G_c}\right] S_c = \frac{W(G_c^2 - G_o^2)}{2g}$$

$$S_c = \frac{W}{2g} \times \frac{(G_c^2 - G_o^2)(G_o + 2G_c)}{(T - D)_e\,(G_o + 2G_c) - 1.5C_cW} \qquad (3)$$

The simplest approximation to $(T - D)_e$ appears to be:

$$(T - D)_e = [(T - D)_o + (T - D)_c]/2$$

and the step-by-step integration indicates this to be a valid approximation since the distance history of $(T - D)$ is practically a straight line. This appears likely to be generally true in view of the following:

(a) The relation of T to V is approximately linear.

(b) A curve of L/D *vs.* C_L is concave upward between any probable values of C_L likely to occur at the end conditions.

(c) The lift, which is equal to W at either end of the maneuver, is equal to $W + F_v$ between these end conditions. Since $D = L/(L/D)$, the effect of this upon D is of opposite sense to that of the shape of the L/D *vs.* C_L curve mentioned under (b).

All of the expressions necessary to predict the take-off transition flight path, which have been developed here, are summarized below:

$$h_c/S_c = 1.5C_c/(G_o + 2G_c) \qquad (1)$$

$$h/h_c = (S/S_c)^N, \text{ where: } N = (G_o + 2G_c)/1.5G_c \qquad (2)$$

$$S_c = \frac{W}{2g} \times \frac{(G_c^2 - G_o^2)(G_o + 2G_c)}{(T - D)_e(G_o + 2G_c) - 1.5WC_c} \qquad (3)$$

where:

$$(T - D)_e = [(T - D)_o + (T - D)_c]/2$$

LANDING—(SEE FIGS. 3 AND 4)

1. h_l/S_l

By a process analogous to that which appears under "Take-off" above, it can be shown that, with the origin at the beginning of the flare:

$$h_l/S_l = -1.5C_g/(2G_g + G_l) \qquad (4)$$

2. $(h_l - h) = A(S_l - S)^N$

Similarly, it can be shown that:

$$N = (2G_g + G_l)/1.5G_g$$

and:

$$h/h_l = 1 - \left(1 - \frac{S}{S_l}\right)^{\frac{2G_g + G_l}{1.5G_g}} \qquad (5)$$

3. Dimensions

Proceeding as under "Take-off:"

$$E_o = (WG_g^2/2g) + Wh_l$$

and:

$$E_l = WG_l^2/2g$$

Then:

$$\Delta E = W\left[\frac{G_l^2 - G_g^2}{2g} - h_l\right]$$

$$(T - D)_e S_l = \Delta E = W\left[\frac{G_l^2 - G_g^2}{2g} - h_l\right]$$

But:

$$h_l = [-1.5C_g/(2G_g + G_l)]S_l, \text{ from Eq. (4)}$$

Therefore:

$$(T - D)_e S_1 = \frac{W(G_l^2 - G_g^2)}{2g} + \frac{1.5C_g}{2G_g + G_l} S_l$$

$$\left[\frac{(T - D)_e(2G_g + G_l) - 1.5WC_g}{2G_g + G_l}\right] S_l = \frac{W(G_l^2 - G_g^2)}{2g}$$

$$S_l = \frac{W}{2g} \times \frac{(G_l^2 - G_g^2)(2G_g + G_l)}{(T - D)_e(2G_g + G_l) - 1.5WC_g} \quad (6)$$

For reasons given under "Take-off," the average of initial and final values appears a good approximation for $(T - D)_e$.

Summarizing, to predict the landing transition flight path:

$$h_l/S_l = -1.5G_g/(2G_g + G_l) \quad (4)$$

$h/h_l = 1 - (1 - S/S_l)^N$, where:

$$N = (2G_g + G_l)/1.5G_g \quad (5)$$

$$S_l = \frac{W}{2g} \times \frac{(G_l^2 - G_g^2)(2G_g + G_l)}{(T - D)_e(2G_g + G_l) - 1.5WC_g} \quad (6)$$

Concluding Remarks

It may be noted that the method neglects such secondary effects as the reduction in induced drag due to proximity to the ground or the gradient with respect to height above the ground which is usually present in the wind velocity. Neither of these effects appears likely to make significant difference in the typical form of the time histories of the accelerating forces, upon the assumed simplification of which the validity of the entire method rests. Allowance for the change in magnitude of the forces due to these effects may be made in the selection of the proper values of $(T - D)_e$ and G to be inserted in the equations. The accuracy of the results of any practical application of the method, however, must depend upon the precision with which the pilot can control the climbing airspeed in take-off or the approach gliding airspeed in landing. For this reason it appears that all such secondary effects may be neglected without introducing significant error. This feature is also common to the generally accepted methods for calculating the flight paths for the other two phases of the complete take-off or landing.

Airplane Vibration Tests as Related to the Flutter Problem

CHARLES B. LYMAN

Bureau of Aeronautics, Navy Department

The Flutter Problem (General)

The flutter problem has been treated analytically by several authors but an attempt will be made in this paper to summarize the general problem as one of the airplane designer and to demonstrate how the airplane vibration test may be employed as a powerful tool in its solution.

The designer's problem is to determine in the early stages of an airplane design the minimum flight velocity at which aerodynamically energized oscillation of a component airfoil surface or combination of surfaces is possible and, to incorporate design features which will assure that this critical flutter velocity will exceed the maximum velocity at which it is intended to operate the airplane. In short he must know (1) what factors governed by design affect the flutter characteristics, (2) how to measure and evaluate these factors and (3) how to determine from the measured values of these factors, with a reasonable degree of accuracy, the value of the critical flutter speed inherent with his design. It cannot be said, however, that there are as yet available completely satisfactory routine methods applicable to calculating the flutter speed of all aircraft components. The airplane designer can, however, by applying basic principles control certain of these measured factors by design so that there is reasonable assurance that the flutter characteristics of the airplane are at least qualitatively influenced in the proper direction.

Nature of Parameters

Analytical treatment, reinforced by controlled laboratory tests as well as correlation with design and service history data has definitely established certain variables as those determining flutter characteristics. These may be broadly separated into: (1) natural frequency of the airplane structural components in pertinent modes of motion; (2) elastic characteristics of the subject structures including location of flexural axes and nodes and loops of vibratory motion; (3) mass distribution characteristics of the structural components including center of gravity location, moment of inertia, mass density and control surface dynamic balance features; and (4) damping characteristics including material damping and friction damping. Of these, only the mass characteristics are readily calculable directly from design data, it being most expeditious to measure the remainder by laboratory tests.

Calculation of Flutter Velocity

The more difficult phase of the problem, namely that of establishing methods and procedures by which the measured parameters may be employed in arriving at a value of the flutter velocity applicable to any given design, has been and is being studied intensively by research and testing personnel. There is every indication that, in the very near future, a designer possessing reasonably accurate values of the flutter parameters applicable to his design will have available methods and procedures by which he either can accurately calculate the critical flutter velocity or he can determine at least whether or not the airplane will be aerodynamically stable throughout the intended range of operating speeds.

Measurement of Parameters

It is hence apparent that the measurement of the flutter parameters is an important and essential problem. It is the primary purpose of this paper, then, to outline the technique of the laboratory vibration test and to describe in what ways it contributes to solving the problem through the measurement of necessary data.

Natural Frequency Determination

Technique

The two principal methods of natural frequency determination are those employing the measurement of amplitude of response to a periodic vibratory force, and the measurement of frequency of free vibration resulting from the application of a step function force. The common phenomenon of response of an elastic member to a periodic applied force is the chief tool in the measurement of natural frequencies. For all intents and purposes, with small system damping such as is the case with aircraft structures, the true natural frequency is very close to the frequency of maximum amplitude response. The observation and measurement of this latter is most convenient and satisfactorily accurate for practically all aircraft vibration testing. Free vibration of structural components is accomplished by the sudden release of applied static loads, the imposition of

Presented at the Airplane Design session, Ninth Annual Meeting, I.Ae.S., New York, January 31, 1941.

Any opinions or assertions contained herein are those of the writer and are not to be construed as official or as reflecting the views of the Navy Department at large.

impact loads, or the discontinuation of periodic applied forces.

Oscillators

A periodic vibratory force may be applied to a structure by means of an oscillator or shaker. Practically all of the shakers used in aeronautical work are of the mechanical variety employing mass unbalance as the source of the applied force. Simple rotary unbalance, double rotary unbalance with elements phased to give periodic translational force or couple, and Scotch yoke unbalance are the common types. A fundamental characteristic of the mass unbalance shakers is that of producing a force of a magnitude proportional to the square of rotary frequency. This necessitates a large unbalance for use at low frequencies and *vice versa*. The unbalance used generally ranges from .065 inch lbs. in a small shaker suitable for control surface excitation to from 2.0 to 4.0 inch lbs. for shakers suitable for exciting engine and fuselage response. The outstanding advantage of the mechanical mass unbalance shaker is its self-contained nature; usually it is attached directly to the body being excited and driven by an electric motor through a flexible drive shaft. No attachment to any rigid reference body is required.

The elastic or so-called "rubber band type" shaker employs an elastic member, one end of which is attached to the structure being excited and the other to an eccentric or Scotch yoke motion. The application of this type is not as simple as for the mass unbalance type as it requires a stationary reference point but it has the capability of producing large forces at low frequencies.

The frequency characteristics of shaker driving mechanisms are very important. Due to the rapid change in amplitude of, and hence also in power absorbed by, a vibrating body near resonance, the oscillator should have suitable speed stability characteristics and ample reserve torque and power to give complete control at frequencies on both sides of the peak.

Amplitude Measurement

The measurement of amplitude may be accomplished in any of a multitude of ways ranging from the simplicity of passing a paper chart under the point of a pencil attached to the subject structure to the relative complexity of the electromagnetic pick-up with its attendant power supply, integrating amplifier and recording oscillograph. The method best suited varies with the application.

The measurement of angular motion is a more difficult problem. It can be accomplished by linear measurements at at least two points disposed in a plane normal to the axis of rotation of the surface. In general, it is necessary to measure the instantaneous relative phase of the two parallel amplitudes in order to quantitatively measure the actual angular motion, as this latter is usually accompanied by some translational motion. The method which best yields this data is the oscillographic recording of the simultaneous output of electric pick-ups properly located. By proper treatment (addition and subtraction) the translation and rotation may be separated. If, however, there is a nodal axis within the structure (that is having no translational motion) the angular motion may be obtained directly from one linear measurement. Since it is often the case that the nodal axis does not fall upon the body, as for the common problem of the measurement of motion of a control surface the hinge line of which is moving translationally, and since the use of electrical equipment if available is always relatively complicated, another method has been developed which yields the desired data in a simpler and yet satisfactory manner. A plane mirror is attached to the rotating surface in a location which preferably has a minimum of translational motion. A light beam is directed from some stationary point onto the mirror and the image reflected upon a fixed screen or ground glass plate bearing a scale and located at a convenient distance from the mirror. The amplitude of the light spot travel is measured on the screen, which amplitude, combined with the distance of the screen from the mirror gives an exact quantitative measure of the angular motion.

Frequency measurement is most conveniently made with an oscillographic system recording the output of an electric pick-up. A well calibrated constant-speed motor driven photographic oscillograph is very satisfactory. A calibrated cathode ray oscillograph also may be employed in combination with electric pick-ups for frequency determination. Stroboscopic devices also are applicable.

Phasing

The phase relationship between the motions of different portions of airplane structures is a very necessary type of data for the proper selection and identification of any given vibration mode. A very simple yet adequate device provides a means of differentiating between "in phase" and "out of phase" motions. Metallic probe points, between which are wired in series a portable battery and lamp, are held adjacent to the two portions of the airplane structure it is desired to phase after electrical bonding between the same has been accomplished. By allowing the probes to make contact (*i.e.*, "tap") once per cycle the relative phase is indicated by whether or not the lamp flashes.

Stroboscopic devices also may be employed. Also, a cathode ray oscillograph, operating upon the output of pick-ups upon the structure at the two points in question will give the phase. The cathode ray will indicate any relative phase as will the stroboscope when used with a common reference motion.

Wing Flutter Mode Natural Frequency Determination

Wing flutter is covered chiefly by four modes, namely: flexural-torsional, flexural-aileron, torsional-

aileron and flexural-torsional-aileron. As is implied by their titles the natural frequency of three different systems is involved: the wing flexural or bending frequency, the wing torsional frequency and the frequency of the aileron control system. In cases where other elastic systems are included in the wing structure, as for example a flap or float installation, other degrees of freedom are correspondingly added and should be considered in combination with those basic degrees of freedom which are pertinent.

Wing Bending

The wing bending frequency of a cantilever monoplane or the wing tip bending frequency of a braced monoplane or biplane is most simply obtained by attaching a shaker at or near the wing tip, located in a chordwise position determined to be near the flexural axis or axis at which an applied force causes only flexure of the structure with no attendant twist. Since the measurement of natural frequency is not critically affected by small variations in this respect the approximate figure of 33 per cent chord is found generally satisfactory. The most important flexural frequency is that of the fundamental symmetrical mode in which the full wing, as a beam, vibrates in a half wave. The mass of the shaker must necessarily be small compared to the mass of the wing so as not to appreciably reduce the resonant frequency below that which would result with no additional mass. This wing mode usually is readily detected by observation but a resonance curve plot of the amplitude of motion at some point aids in the accuracy of detection. Many analytical treatments of the flutter motion in which this mode is considered treat the wing as a cantilever fixed at the airplane center line. It is found, however, that the actual motion possesses symmetrical node locations somewhat outboard of the center line with finite vertical motion existing in the fuselage in way of the wing. The location of these nodes of course affects the resonant frequency and hence if there are supporting forces present forcing nodes at points other than those applicable to the desired mode, the measured resonant frequency will differ from that strictly applicable. Fortunately, it has been found that in the case of a conventional landplane this is not a large source of error in that node locations observed with the airplane, suspended upon a relatively soft sling, thus simulating somewhat free suspension, do not differ significantly from those obtained with the airplane resting upon its landing gear. It is considered, however, that the use of a proper sling is the better arrangement especially for float seaplanes which can otherwise be supported only very rigidly at the center line by means of handling trucks.

The flexural natural frequency also can be excited by means of applying a shaker to the fuselage and observing or measuring the frequency of resonant tip motion in a similar manner. In this method, a larger shaker must be employed, and it is usually convenient to attach the shaker at the engine. In this way, the fuselage mode accompanying the desired wing mode can be studied. It should be pointed out that as soon as other elastic structural members are excited in series (so to speak) with the surface in question such as is the case when the wing is excited from the engine through the fuselage, the resulting motions become more complex and the possibility of selecting a fallacious natural frequency due to the resonant response of a connected structure becomes more imminent.

Natural wing bending frequency also can be obtained by the frequency measurement of free vibration excited by imposing an impact load at the tip, releasing a static load or stopping a shaker attached to the structure. Higher frequency wing bending modes, both unsymmetrical and symmetrical, can be studied in a similar manner by shaker excitation.

Wing Torsion

The most important natural frequency concerned in the wing flutter study is that of wing torsion. The significant mode is the fundamental in which chordwise wing sections twist about some axis of oscillation forming an approximate one-quarter wave outboard of a node near the airplane center line with the maximum amplitude occurring at the tips. This mode may be excited by means of an oscillator and the resonant frequency observed or selected from a resonance curve of angular motion; or the frequency of a free vibration resulting from the release of an applied force or couple may be obtained with frequency measuring equipment.

When using the resonance method, the applied shaker excitation should be such as to produce as pure a torsional motion as is possible. For this reason it has been necessary to employ linear force vibrators located offset from the axis of rotation far enough to produce as high a ratio of couple to bending shear as possible. This may be accomplished by attaching the shaker to the trailing edge structure or to a boom rigidly clamped or attached to the wing beam or fittings and extending forward or aft from the surface. If the shaker is attached to the trailing edge care must be exercised so as to insure that the rigidity of the structural carry through to the main torque carrying member is sufficient to preclude local resonance and a fallacious value for the observed natural frequency. If a torsional boom is used, it must be designed also to be sufficiently rigid to eliminate bending resonance and should at the same time be light, with its mass disposed so as to add a minimum of moment of inertia to the chordwise section.

The torsional frequency of a braced biplane wing cellule may best be excited by applying a shaker to the interplane bracing so as to act in a fore and aft direction and displaced vertically from the effective torsional spanwise axis. In this way, the vertical bending mode response is avoided, there being negligible fore and aft response due to the inherent high rigidity in this direction. Similarly, in applying shaker excitation to a

monoplane wing, if the boom employed extends vertically above or below the surface, the same advantages will result. Coupling with the wing bending may also be eliminated by supporting the wing along the desired nodal axis thus forcing the desired mode.

The natural bending and torsional frequencies are affected by the disposition of concentrated masses such as items of equipment, armament or landing gear especially those located well outboard and either having their masses disposed longitudinally or their center of gravity positions displaced a considerable distance from the elastic axis. For this reason the flutter characteristics of an airplane may vary considerably with different conditions of loading. Likewise noticeable is the change of natural frequencies resulting in a convertible airplane with a change from landplane to seaplane type gear. Here the tip floats, located well outboard and below the wing, considerably depress the natural frequencies. For such a case the bending frequency may be obtained in the same manner as with no tip float, but it is easier to excite the torsional mode by applying a shaker to the float or float bracing structure so that the force is directed fore and aft. To check for the effect of the flexibility of the float bracing in both the fore and aft and transverse directions as related to observations of resonant frequencies of wing torsional and bending response, respectively, the wing should be supported at the float bracing attachment points, and the natural frequencies of the float determined relative to the wing so fixed.

Aileron System

The aileron system, consisting of control surfaces, horns, bell cranks, push rods, cables and cockpit controls is a complicated combination of various masses, flexibilities and kinematic relationships. The mode of motion of interest in the flutter consideration is that of angular motion of the surface about its hinge line when restrained elastically by its control system. The important mode is a symmetrical one which is independent of the restraint supplied at the control stick, this being a node, and in which each aileron vibrates as a part of the elastic system formed by the controls on its side of the airplane. The natural frequency may be determined by employing shakers or by studying free vibration. A small mechanical shaker attached to the trailing edge of one aileron will satisfactorily excite the desired mode. It is found that no significant difference in observed symmetrical mode resonant frequencies results with the control stick free, hand held, or braced rigidly to the fuselage structure. It is convenient, however, to facilitate the measurement of vibratory response amplitudes by eliminating the superposition of extraneous angular excursions of the system by securing it rigidly in the cockpit.

The problem of the increase in moment of inertia of the surface due to the addition of the shaker mass becomes proportionally more important in the case of the aileron inasmuch as, with indiscriminate use of heavy shakers on small control surfaces, the resonant frequency observed will be considerably below the proper system natural frequency. To correct for the additional mass contributed by the shaker, the resonant frequency of the system may be determined with several different amounts of additional mass, the results plotted logarithmically and an extrapolation made for the known amount of the shaker mass. This method may be used also in lieu of knowledge of the surface moment of inertia.

With the controls restrained, a lower frequency unsymmetrical mode of vibration is observed in which the surfaces oscillate out of phase (*i.e.*, one up and the other down) with some motion occurring at the stick. This frequency usually varies with the restraint, however, and is not considered as significant in the flutter problem. When flutter calculations are made for the mode involving unsymmetrical aileron motion, the conservative assumption of zero natural frequency is made. Measurements of angular surface motion are obtained easily by the previously described mirror-light beam method.

Ordinarily, the aileron system natural frequency is considerably lower than that of wing torsion so that coupling between the two modes is negligible. The bending frequency, however, is more likely to be close enough that it may be necessary to support the wing against deflection so as to eliminate coupling and the consequent shift of natural frequency from uncoupled values. It is noted that the reflected light beam method of angular measurement, when properly employed, differentiates between angular and linear displacements and is not influenced by the presence of the latter.

Tail Flutter Mode Natural Frequency Determination

Tail Surface Modes

The tail flutter modes involve both the coupling of the fixed and movable control surfaces in different degrees of freedom and the coupling of the tail surface with the various modes of the fuselage structure. Interaction of symmetrical bending of the horizontal fixed surfaces with oscillation of the elevator system can occur in much the same way as wing bending-aileron flutter. Also, horizontal tail surface modes comparable with the wing flexure-torsion and torsion-aileron are within possibility but do not represent highly probable conditions. Transverse bending of the fin coupled with oscillation of the rudder system is a further consideration. A determination of the natural frequencies of the stabilizer bending and torsion, of the fin in bending, and of the elevator and rudder systems supplies such necessary frequency data for the investigation of these modes.

Stabilizer

The bending frequency of the stabilizer is most easily obtained by mounting a shaker on or near the tip and observing resonance. As with the wing, care must be taken in locating the shaker so that coupling of the desired mode with other modes is minimized. Also with small surfaces, in which the weight of the shaker is considerable relative to that of the surface itself, it may be necessary to apply it near the root, shaking the fuselage attachment points vertically so as to excite the proper flexural mode without the addition of excessive mass at the tips where it is very effective in reducing the resonant frequency. However, every resonant mode as shown by a resonance curve of amplitude measured at a point on one side of the fuselage must be completely investigated by means of an amplitude and phasing survey to insure that the proper frequency is selected. By this means, other modes such as fuselage vertical bending, fuselage torsion, fin bending, unsymmetrical stabilizer bending, or motion resulting from local flexibility of fuselage attachment points can be identified. By supporting the conventional landplane upon its landing gear (including tail wheel) the vertical bending frequency of the fuselage is eliminated. If such local support of the tail is not feasible, the resonance frequencies obtained in the measurement of stabilizer motion must be carefully compared with those obtained in the measurement of fuselage motion at the tail in order that the proper frequency resulting in maximum ratio of stabilizer tip to stabilizer root motion may be selected. The stabilizer natural frequency also may be determined from observations or measurements made while supporting the airplane from a sling and applying a shaker at the fuselage location corresponding to the engine. However, as previously mentioned, the possibility of selecting a fallacious natural frequency due to the resonant response of some structure located between the shaker and the tail is much more probable.

The torsional natural frequency of the stabilizer, usually very high in the conventional tail with its conventionally low aspect ratio and short span, is accordingly more difficult to excite and detect by shaker excitation. The methods of applying shakers offset from the nodal axis either by attaching directly to the surface or to suitable booms is applicable.

Fin

The fin bending frequency is similarly obtained by attaching a shaker to the fin tip so as to produce a force in a transverse direction and observing or measuring fin transverse amplitudes. In a manner similar to the technique described for the determination of the stabilizer bending frequencies, the same precautions must be taken of identifying the exact nature of all modes of resonant transverse response of the fin so as to differentiate the fin bending from the other related modes which also result in such motion.

Elevator and Rudder Systems

The natural frequency of angular oscillation of the elevator or rudder about its hinge line as elastically restrained by the control system is the important consideration. This is obtained by attaching a shaker offset from the hinge line, preferably near the horn attachment points so as to eliminate torsional oscillation of the surface itself.

The elevator and rudder systems differ from the aileron system in that the elasticity and masses are not symmetrically disposed about the cockpit controls so as to cause the natural frequency of surface motion due to the elasticity of the system in the fundamental mode to be necessarily independent of the external restraint provided at the cockpit controls. Depending upon the kinematic and mass disposition characteristics of the control system itself, the actual method of restraint at the cockpit controls may or may not affect the value of the resonant frequency. The method of restraint most applicable is that which would be provided normally by the pilot. In any event the frequency goes up with the rigidity of restraint and the upper limit is represented by the condition wherein the cockpit controls are rigidly braced to the fuselage structure at the point where the control force is normally applied by the pilot. Conversely, the case of minimum restraint is that obtained with free controls. The possible range of natural frequencies will hence lie between the limiting values obtained by these test conditions.

Tail Surface-Fuselage Modes

Those possible tail flutter modes in which the motion of the fuselage constitutes one of the degrees of freedom include:

(a) Fuselage torsion-rudder system: in which dynamic mass unbalance of the rudder surface referred to its own axis and the effective nodal axis of fuselage torsional motion, causes coupling of the two modes.

(b) Fuselage vertical bending-elevator system: in which the vertical motion of the tail portion of the fuselage is coupled with oscillation of the elevator system by lack of dynamic balance of the latter.

(c) Fuselage transverse bending-rudder system: which is strictly analogous, to the above mode with motion occurring normal to rather than in the plane of symmetry of the airplane.

(d) Fuselage torsion-elevator torsion: in which torsional deflection of the elevator, unsymmetrical with respect to the airplane center line is induced from fuselage torsional motion through dynamic unbalance of each half of the elevator surface relative to the hinge and fuselage torsional axes. If there is a local flexibility of the stabilizer relative to the fuselage about a fore and aft axis through the attachments, it is considered that this mode may be substituted for the fuselage torsional mode in that it produces the same type of elevator hinge line motion.

It is to be noted that all of these tail flutter modes

have been described as having two degrees of freedom. However, just as with wing flutter, those modes with more degrees of freedom are the more general possibilities. Hence for example fuselage transverse bending-fuselage torsion-rudder system flutter may be a consideration.

Fuselage Modes

The natural frequencies of vertical and transverse flexure of the fuselage structure are those at which resonant response at the tail in the pertinent direction results from excitation of the fuselage causing it to vibrate as a whole. They can be interpreted also as those frequencies of excitation at which the tail location occurs at a loop of the fuselage elastic curve. These data are best obtained by applying a large shaker to the airplane (most conveniently at the engine) and measuring the amplitude response at the tail. The resulting resonance curves, after complete identification of the airplane mode occurring at each peak, will indicate the proper fuselage natural frequencies pertinent to tail flutter. When vibrating vertically, the amplitude should be measured vertically on the airplane center line at or near the main stabilizer beam. When excited by a transverse shaker force, the amplitudes should be measured transversely at the main fin beam at a vertical position which has been determined by preliminary survey to be the node of any torsional motion which may be induced. The airplane should preferably be freely supported in a sling for such vibration tests. To eliminate extraneous control surface motion, the cockpit controls are best restrained rigidly.

The natural frequency of the empennage in torsion as elastically restrained by the fuselage can most directly be obtained by applying a shaker on the tail offset from the nodal axis so as to exert a force either transversely at the fin tip or vertically at the stabilizer tip. That resonant frequency of fuselage torsional amplitude is selected which a knowledge of related tail surface natural frequencies and a complete phasing identification of fin and stabilizer tip motions shows to be the applicable mode. The tail should be freely supported for such an investigation but it has been found in many cases that the resting of a landplane tail wheel upon the floor did not alter the value of the observed torsional natural frequency. It has been noted also that in the case of some airplanes having tubular fuselage construction in which a vertical section is a tall rectangle and which have different transverse rigidities in the upper and lower panels, that more than one natural torsional mode results.

Elevator Torsion

In this mode the opposite sides of the elevator oscillate in an approximate quarter wave unsymmetrically about the airplane centerline as a node. The elevator in a conventional system is connected by a continuous torque carrying member and the connection to the control system is made at or near the airplane center line where the node occurs. Hence in order to excite this mode, the shaker should be located offset from the hinge line near one tip, and the horn should be preferably restrained. However, if the subject natural frequency sufficiently exceeds that of the symmetrical mode of the system, the error due to coupling with control system elasticity will be small. If the excited torsional twist of the elevator tip is too small for accurate observation, the use of the reflected light spot method of angular measurement is convenient. The unsymmetrical mode should not be confused with the symmetrical torsional mode in which the tips twist in phase accompanied by an opposite twist of the central portion. This occurs at a higher frequency.

Determination of Elastic Characteristics

Certain of the elastic characteristics of aircraft structural components which are necessary for use in the investigation of flutter speeds are measurable in the laboratory. This consists of completely determining the deflection or elastic deformation characteristics of the structure in the various modes which are concerned in possible flutter motions. Included is the determination of the nature of the elastic curves resulting both at zero frequency of applied force or couple and at a frequency corresponding to the natural frequency. When the designer uses certain natural frequencies in his flutter calculations he should consider fully the manner in which they were obtained, whether they are for coupled or uncoupled modes, where the nodal axes are located, and how such locations compare with that of the flexural axis.

The elastic or flexural axis has been defined as that axis about which the surface rotates under the application of a pure static couple. It is also defined as the chordwise position at which an applied static force will produce only pure translational displacement of the surface. The location of this axis may be determined by two methods—those implied by the alternate definitions. A pure couple may be applied near the tip section and measurement made of the locus of chordwise points which undergo no displacement. Alternately, a force may be applied in successive chordwise locations at each wing section and that location observed at which the vertical displacement of leading and trailing edges are identical. The wing must be securely supported and the measurements made accurately in order to produce useful data. Coincident with the former method, a measure of torsional stiffness useful in divergence speed calculations may be obtained from the known values of applied couple and measured values of torsional deflections.

A very important use for the knowledge of nodal axis locations concerns all modes involving control surface flutter and that is its use as the basis for dynamic balance requirements for the surfaces. An axis of

torsional fuselage motion observed in the laboratory is a much safer basis for dynamic balance calculations for the rudder than an arbitrary center line of thrust location or center line of supporting structure. Node locations of fuselage bending observed in the laboratory will be the most logical and conservative bases for balance calculations inasmuch as their selection will have taken into account the actual elastic characteristics of the given structure including the effect of cut outs.

The actual flexural mode of a surface such as a wing or horizontal tail directly affects the natural frequency. If "unnatural" node locations are forced due to rigidity of supports, "unnatural" natural frequencies result. If the node location is artificially forced at the wing root such as would be obtained by rigidly supporting the fuselage or by use of a jig, the natural frequency is lowered. Also, if nodes are artificially forced outboard of their natural location by rigid supports or by support by landing gear running to outboard points on the wing, the natural frequency is likewise lowered.

Determination of Mass Characteristics

Of the pertinent mass characteristics involved in the flutter consideration, none are primarily determined by laboratory tests as analytical calculation ordinarily produces sufficiently accurate data. The function of the laboratory test in checking such calculated data, however, merits some mention.

Center of gravity or inertia axis positions of fixed surfaces can be checked approximately by the location of the nodal axis in the torsional frequency determinations as previously mentioned. Movable control surfaces can be removed and readily checked for *c.g.* position. By swinging on a calibrated torsional pendulum the moment of inertia may be determined. A method is also available for laboratory quantitative determination of product of inertia by forced high frequency oscillation of the surface about one axis and observing the location of nodes resulting in the motion induced about the other axis.

Determination of Damping Characteristics

Internal structural damping is an important factor influencing the flutter phenomenon. It is known that an increase in the damping characteristics of any elastic system concerned in flutter will raise the critical velocity at which flutter is encountered. In the absence of data concerning applicable values of damping characteristics it is conservative to calculate the flutter speed assuming zero damping. However, the difference in calculated speeds between an assumption of zero damping and one of a small amount of damping may in some cases be great. Hence, if zero damping leads to a flutter speed value not sufficiently high, it is reasonable that the designer is concerned with determining values of the damping characteristics which are applicable to his design and which will result in a reasonable yet conservative value of flutter speed.

It is important to note that in the analytical treatments of flutter the aerodynamic forces and moments upon the airfoil in its non-steady motion are completely expressed so as to include the oscillatory component of motion, and hence the damping coefficient correctly applicable to the calculations must represent only the internal dissipative forces and should not include any of the aerodynamic damping necessarily encountered in the oscillation of an airfoil in the atmosphere either at rest or at any forward velocity. Most of the laboratory methods of measuring damping unfortunately involve dynamic vibratory tests and hence include aerodynamic effects.

Internal structural damping may be evidenced as (1) creep or plastic flow, (2) elastic hysteresis or deviation of a homogeneous material from linear elasticity, exemplified by the area enclosed by a stress-strain curve and (3) friction or relative motion of parts of a non-homogeneous structure usually occurring in bearings or mechanical joints. The inherent nature of aircraft structural materials eliminates the first from consideration. The effective combination of the latter two types may be evaluated by obtaining a load-deflection curve for the subject structure as it is taken slowly through a complete cycle of reversal of load. Because of the very low damping of a typical aircraft structure, extreme accuracy of measurement of load and deflection is essential. The loading should be such as to produce a deflection curve approximating that of the mode under consideration. It is considered that concentrated loads produce a satisfactory approximation for the fundamental modes. The damping coefficient may be evaluated from the energy represented by the area enclosed in the elastic hysteresis curve, the spring constant of deflection at the measured point and the maximum amplitude of cyclic deflection.

Damping may be determined from displacement-time curves of free vibration obtained by the sudden release from an initial deflection or the sudden removal of a vibratory shaker force occurring at a frequency near that of free vibration. Damping may also be determined in several ways from resonance curves of motion of the structure in the pertinent mode. The damping coefficient can be determined from certain well known relationships involving the phase angle between vibratory force and actual displacement as measured at frequencies bearing certain definite relationships to the resonant frequency. The ratio of the maximum response at resonance to the static deflection that would be obtained under an applied load equal to that exerted by the shaker at resonance is also an inverse measure of the damping.

It is acknowledged that some of these relationships indicated above apply only to systems having low orders of damping, but it is considered that aircraft structures are satisfactorily included within this classification.

Institute Notes

Institute Meetings

Wednesday, December 17, 1941

Wright Brothers Lecture. "New Pathways in Aeronautical Theory," by Prof. Richard V. Southwell, Professor of Engineering Science, Oxford University, England. At the Pupin Physics Laboratories, Columbia University, New York City; 8:30 p.m.

Dinner to Wright Brothers Lecturer. At Columbia University Faculty Club, New York City; 6:30 p.m.

Tuesday, January 27, 1942

Honors Night Dinner. At the Hotel Waldorf-Astoria, New York City; 7:30 p.m.

Wednesday–Friday, January 28–30, 1942

Tenth Annual Meeting. Annual Business Meeting of Members, Wednesday, January 28, 5:00 p.m. Three days of technical sessions—morning, afternoon and evening—on Aerodynamics, Airplane Design, Air Transport, Materials, Meteorology, Physiological Problems, Power Plants, Radio and Instruments, Rotating-Wing Aircraft, Structures.

The dates and hours for the various technical sessions will be announced in the December issue of the Journal together with the titles of the papers to be presented. A large number of papers have already been received and submitted to the Chairmen of the sessions concerned, who will shortly make the final choice of the papers to be presented at their sessions. However, any members who have prepared technical papers or contemplate doing so are still urged to send their papers or outlines to the Institute. Even if it should be found impossible to include their papers in the appropriate session at the Annual Meeting, the session Chairmen and the Editorial Board would like to have these papers to be considered for presentation at meetings of Institute Sections or for publication in the Journal.

New Corporate Members

The Institute is pleased to announce the following new Corporate Members:

American Bosch Corporation, Springfield, Mass., manufacturers of magnetos for four-, seven-, nine-, fourteen- and eighteen-cylinder aircraft engines. The company also manufactures fuel injection equipment.

Dowty Equipment Corporation, Long Island City, N. Y., manufacturers of the "Live-line" automatic hydraulic pump, the levered suspension type landing gear strut manufactured under license of Dowty Equipment Ltd. of England, actuating cylinders, valves and allied equipment. The company is also engaged in the development of a new type landing gear for the Air Corps.

News of Institute Members

Glenn D. Angle, A.F.I.Ae.S., Editor of the aviation yearbook "Aerosphere" and consulting engineer on aircraft engines, has organized at Tecumseh, Michigan, the Angle Engineering Company of which he is Vice-President and Chief Engineer. The company will be engaged in the design, development and manufacture of internal combustion engines, principally for aircraft.

Gerald H. Backer, M.I.Ae.S., has joined the faculty of the College of Engineering, University of Kentucky, as Assistant Professor of Aeronautical Engineering. He had previously been Instructor in Engineering at the Casey Jones School of Aeronautics and Academy of Aeronautics since 1934.

Edward E. Brush, M.I.Ae.S., has become Associate Professor and Head of the Department of Aeronautical Engineering at the University of Kansas. He had been a Senior Project Engineer for Lockheed Aircraft Corporation and before that an Instructor in Aeronautical Engineering at the University of Minnesota.

Pilot Officer C. G. Bull, Technical Member, formerly Mechanical Engineer with the Royal Canadian Air Force, is now assigned to flight instruction on advanced aircraft in the R.C.A.F.

Adolph Burstein, M.I.Ae.S., Project Engineer with Vultee Aircraft, Inc., has transferred from the Stinson Division in Michigan to the company's main plant in California.

Col. V. E. Clark, F.I.Ae.S., has been appointed a member of the National Panel of Arbitrators of the American Arbitration Association, according to announcement of its President, **C. V. Whitney,** M.I.Ae.S. This organization expedites the settlement of commercial and industrial controversies through arbitration. Colonel Clark, now technical consultant to Hughes Aircraft Company, has been prominently active in the aeronautical engineering field since 1915 when he was Chief Aeronautical Engineer for the U.S. Army Air Services. He is well known for his development of the "Clark Y" series of airfoils as well as for more recent work on the design of many types of aircraft, including plastic molded airplanes.

Herbert F. DeWeese, Technical Member, formerly Engineer and Aircraft Instrument Instructor at the Lincoln Airplane & Flying School, is now Instrument Installation Design Engineer with the Wichita Division of Boeing Aircraft Co.

Herbert M. Heuver, M.I.Ae.S., has joined the Experimental Engineering Section, Materiel Division of the U.S. Army Air Corps at Wright Field as an Aeronautical Engineer. Except for a three-year period in 1937–39, Mr. Heuver has been an Engineer with the University of Washington since 1933. He designed the wind tunnel and other aeronautical equipment there in collaboration with **Prof. F. K. Kirsten,** A.F.I.Ae.S., and was in charge of the research work conducted by the Aeronautical Department.

Evert C. Hokanson, M.I.Ae.S., has been appointed to represent the Aviation Department of the Whiting Corporation, Harvey, Illinois, in their recently opened West Coast office. Mr. Hokanson was previously engaged in the development of aircraft performance standards and standard flight test procedures for the Engineering Flight Test & Inspection Section of the C.A.A. He has had experience as an Aeronautical Engineer with United Air Lines, Hall Aluminum Aircraft Company and Boeing Aircraft Company.

Roger F. Horton, Technical Member, formerly an engineer with the Acrotorque Company, has been Chief Inspector for Dowty Equipment Corp. since June of this year.

D. C. Jackson, Jr., M.I.Ae.S., has taken a year's leave of absence from the University of Notre Dame where he has been Dean of the College of Engineering and Professor of Mechanical Engineering since 1939. He will go on active duty as a Major in the U.S. Army and will be stationed at Frankford Arsenal in Philadelphia. Major Jackson was a Lieutenant in the U.S. Army during World War I. He has devoted his entire time, since receiving his S.M. degree from M.I.T. in 1922, to engineering education. This included posts as Director of Lewis Institute in Chicago, Head of the Electrical Engineering Department at the University of Kansas, and Head of the Department of Mechanical and Electrical Engineering at the University of Louisville.

Sgt. Pilot Desmond F. Macdonald, Technical Member, has completed his Student Pilot course in the Royal Canadian Air

Force and is now a Staff Pilot of the Second Bombing and Gunnery School.

Capt. S. G. Nordlinger, Technical Member, recently promoted from rank of 1st Lieutenant, is with the U.S. Army Air Corps Materiel Division at Wright Field doing experimental work on aircraft engines and accessories. He was formerly Chief Test Engineer, Detroit Division, Continental Motors Corp.

James D. Redding, A.F.I.Ae.S., Formerly Assistant Chief of the C.A.A. Aircraft Airworthiness Section, is Staff Representative for Aeronautics with the Society of Automotive Engineers.

George Tharratt, M.I.Ae.S., was recently appointed Chief Engineer of Adel Precision Products Corp. in Burbank. He brings to this new position twenty years of experience in aircraft design and production in England, Canada and the United States. For the past two years he was Supervisor of the Department of Production Engineering which he formed at the Douglas Aircraft Company. During his association with Douglas, which he joined in 1936 as an airplane designer, he also organized a section to design and create interior furnishings for commercial transport planes. Previous to this he was an engineer with Great Lakes Aircraft Co. and The Glenn L. Martin Co.

Frederick R. Weymouth, A.F.I.Ae.S., has joined the Department of Design Engineering of Bell Aircraft Corporation. He was recently Assistant Professor of Aeronautical Engineering at New York University and for the ten years preceding had been in the Engineering Departments of Curtiss-Wright Corporation at their Buffalo and St. Louis plants.

Eli A. Zeitlin, Technical Member, has left the staff of the N.A.C.A. at Langley Field, where he was a Junior Engineer, to take a position as Assistant Aeronautical Engineer in the Bureau of Aeronautics, Navy Department.

Sections

Los Angeles. Wing Commander Michael Crosley, representing the British Air Commission at the North American Aviation plant, was the guest speaker at a dinner meeting of the members in the Los Angeles region held on October 14. Wing Commander Crosley is now a Test Pilot for the Royal Air Force, but had previously been a Fighter Pilot and has 35 victories to his credit. He is an authority on the subject of war in the air and spoke to an interested audience of over 250 Institute members on his experiences.

New York. On October 8, a dinner meeting was held at the Advertising Club in New York City. This first meeting of the season for members in the Greater New York area was attended by 160 members and guests. After dinner, Victor J. Skoglund, Project Engineer of Pratt & Whitney Aircraft, read his paper on "Icing of Carburetor Air Induction Systems of Airplanes and Engines," which was illustrated with slides. This paper is published in full in the October issue of the Journal. T. P. Wright, Past President of the Institute and formerly Director of Engineering for the Curtiss-Wright Corporation, gave a talk on "The Aircraft Program of the OPM and Other National Defense Agencies." Mr. Wright is now Assistant Director of the Aircraft Section of OPM. He gave an interesting account of the mutual problems faced by industry and government in the National Defense effort and the plans and procedures for their solution. His talk was followed by a lively discussion period.

The Committee in charge of the meeting was composed of Dr. R. P. Harrington, Polytechnic Institute of Brooklyn, Prof. F. K. Teichmann, New York University, and Walter M. Hartung, Casey Jones School of Aeronautics. Dr. Harrington was Chairman of the meeting.

Student Branches

Aero Industries Technical Institute. New officers for this Branch are: Edwin Gustafson, Chairman; Samuel Burton, Vice-Chairman; Philip Hier, Secretary-Treasurer. At a recent meeting, William Douglas of the Douglas Aircraft Company spoke on plant experience.

Agricultural and Mechanical College of Texas. The first meeting of the school year 1941–42 was held on September 23 at which Prof. Howard W. Barlow, Honorary Chairman, presided. Officers were elected as follows: Roy Grobe, Chairman; R. Skidmore, Vice-Chairman; S. Kaffer, Secretary; and John Pratt, Treasurer. On October 9, Edgar Lesher read the Student Branch Lecture on "Typical Research Problems of United Air Lines" by R. D. Kelly.

University of Alabama. Officers for the 1941–42 school year are: Angelo Conti, Chairman; Andrew Kuzmik, Vice-Chairman; and George Alderdice, Secretary-Treasurer.

Boeing School of Aeronautics. At a meeting held on September 3, officers were elected as follows: Raymond Tuthill, Chairman; Robert Crowther, Vice-Chairman; Stanley Soult, Secretary-Treasurer. Dr. Maurice Garbell is Honorary Chairman.

Indiana Technical College. On October 1, at its first meeting, officers for this Student Branch were elected as follows: Alan Starr, Chairman; William Hazard, Vice-Chairman; Norman Cosner, Secretary-Treasurer. Prof. James Ross is Honorary Chairman.

North Carolina State College. A smoker was held on September 30, the first meeting of the school year, at which Prof. L. R. Parkinson, head of the Aeronautics Department, was guest speaker. Officers were elected as follows: W. S. Johnson, Jr., Chairman; J. R. Weaver, Jr., Vice-Chairman; A. Michaels, Secretary-Treasurer.

University of Notre Dame. Officers for this Branch are: John L. Hoelscher, Chairman; William Ungeschick, Vice-Chairman; Robert S. Mullaney, Secretary-Treasurer.

Rensselaer Polytechnic Institute. Capt. W. M. Masland, Atlantic Division, Pan American Airways, spoke informally at a meeting held on October 9. The meeting was attended by approximately 200 members and guests.

Personnel Opportunities

The Personnel Bureau serves individual members, as well as organizations seeking to employ aeronautical specialists. Any member or organization may have requirements listed without charge.

Wanted

Layout Draftsmen. Nationally recognized aircraft plant east of the Mississippi—a volume manufacturer of planes even in normal times—desires experienced layout draftsmen. Please list your experience and salary required. Address reply to Box 142, Institute of the Aeronautical Sciences.

Two Project Engineers and Several Aircraft Layout Draftsmen. Middlewest. Permanent posts to suitable men. In reply please give academic training, previous experience and salary desired. Address reply to Box 143, Institute of the Aeronautical Sciences.

Changes in Membership

The following changes in the membership of the Institute have occurred since the publication of the previous issue of the Journal.

Elected to Member Grade

Cone, John Carrol, Asst. Vice-Pres., Pan American Airways System, Inc.

Doane, Foster Baird, B.S. in Chem. Eng.; Vice-Pres. and Treas., Maganaflux Corp.

Nelson, Donald Earl, M.S. in Ae.E.; Stress Analysis Engineer, Northrop Aircraft, Inc.

Vanderlipp, Nathan Floyd, Chief Engineer, Fairchild Aircraft Ltd., Canada.

Transferred to MEMBER Grade

Smith, Appollo Milton Olin, M.S. in Ae.E.; Asst. to Chief Aerodynamicist, El Segundo Div., Douglas Aircraft Co.

Elected to Industrial Member Grade

Fowler, Robert Erwin, Public Relations Director, Air Associates, Inc.

Litchfield, Burnham, Vice-Pres. and Gen. Mgr., Allied Aviation Corp.

Potter, Charles Allison, Aviation Representative, The Texas Co.

Elected to Technical Member Grade

English, John Morley, B.A.Sc.; Resident Technical Officer, British Air Comm., Lockheed Aircraft Corp.

Pfaff, George Charles, Jr., B.S.; Stress Analyst, The Glenn L. Martin Co.

Pierce, Ernest William, M.A.; Aerodynamics Dept., Douglas Aircraft Co.

Small, Ronald J., B.S. in M.E.; Research Engineer, Brewster Aeronautical Corp.

Transferred from Student Member to Technical Member Grade

Allen, Glenn Merrill, B.S. in Ae.E.; Engineer, Airplane Div. (Columbus Plant), Curtiss-Wright Corp.

Allison, James Robert, B.S. in G.E.; Engineer, Propeller Dept., Engineering & Research Corp.

Amico, Gaetano Vincent, B.Ae.; Engineer, Airplane Div. (Columbus Plant), Curtiss-Wright Corp.

Anderson, Joseph Lorain, B.S. in Ae.E.; Jr. Aero. Engineer, Ames Aero. Lab., N.A.C.A.

Archer, Gerald Raymond, B.Ae.E.; Draftsman, The Glenn L. Martin Co.

Armbrust, Charles M.

Armstrong, Alfred P., Draftsman, The Glenn L. Martin Co.

Barton, Allen Brown, B.S. in Ae.E.; Engineering Aide, Naval Aircraft Factory.

Barzda, Justin Joseph, Jr. Draftsman, Vought-Sikorsky Aircraft Div., United Aircraft Corp.

Barzelay, Martin Elwood, M.S.; Chief Stress Analyst, Cluett Aircraft Co.

Batchelor, Burton Hazen, B.S. in Ae.E.; Jr. Engineer, Ames Aero. Lab., N.A.C.A.

Becker, Richard Karl, Draftsman, Vought-Sikorsky Aircraft Div., United Aircraft Corp.

Belitz, Hans Gunter, Jr. Aero. Engineer, U.S. Army Air Corps, Wright Field.

Bernstein, Allen Irwin, Stress Analysis Engineer, Airplane Div. (Buffalo Plant), Curtiss-Wright Corp.

Bockmann, Wilbur Howard, B.Ae.E.; 2nd Lt., U.S. Army Air Corps.

Boetel, Victor Frank, B.S. in Ae.E.; Jr. Stressman, Fairchild Aircraft Div., Fairchild Engine & Airplane Corp.

Box, William Albert, B.S. in M.E.; Engineering Trainee, Lockheed Aircraft Corp.

Brazier, Joseph Grant, S.M. in Ae.E.; Aero. Engineer, Douglas Aircraft Co.

Breitenbach, Max J., B.S. in Ae.E.; Aero. Engineer, Consolidated Aircraft Corp.

Brodie, Donald Franklin, Engineer, Shop Contact, Airplane Div. (Buffalo Plant), Curtiss-Wright Corp.

Brown, Clarence Blair, Jr., Draftsman, The Glenn L. Martin Co.

Brown, Edmund Daboll, S.M. in M.E.; Project Engineer, Pratt & Whitney Aircraft Div., United Aircraft Corp.

Burns, Meryl C., Meteorology Instructor, Navigation Section (Univ. of Miami), Pan American Airways System.

Butt, Charles Stahle, Jr., B.S.; 2nd Lt., Experimental Engineering Section, U.S. Army Air Corps, Wright Field.

Cornell, Wellington Curtis, B.S.; Draftsman, The Glenn L. Martin Co.

Curry, Robert Cooper, Instructor in Aero. Engineering, Casey Jones School of Aeronautics.

Dickson, Arthur Frederick, Inspector, North American Aviation, Inc.

Donnell, Ralph Harding, B.S. in M.E.; Jr. Engineer, Grumman Aircraft Engineering Corp.

Doty, Louis Francis, Ae.E.; Instructor in Aeronautics, Ground School, U.S. Naval Air Station, Jacksonville, Florida.

Doudna, Robert Francis, B.S. in E.E.; Jr. Flight Instrumentation Engineer, Boeing Aircraft Co.

Dunbar, William Rice, B.S. in Ae.E.; Student Engineer, Douglas Aircraft Co.

Elliot, Roger Douglas, B.Ae.E.; Engineer, Pratt & Whitney Aircraft Div., United Aircraft Corp.

Fischer, Walter William Alvin, B.Ae.E.; Meteorologist, United Air Lines Transport Corp.

Forward, Delbert James, Ae.E.; Engineer, United States Aeromotive Corp.

Franklin, Peter Gordon, Instructor, Curtiss-Wright Technical Institute.

Gahm, Herman, Instructor, Casey Jones School of Aeronautics.

Ganzer, Victor Martin, B.S. in Ae.E.; Jr. Research Engineer, Ames Aero. Lab., N.A.C.A.

Graham, Donald Joseph, B.S. in M.E.; Jr. Aero. Engineer, Ames Aero. Lab., N.A.C.A.

Graninger, Howard Joseph, B.S. in M.E.; Jr. Engineer in Exp. Eng. Test, Wright Aeronautical Corp.

Hall, Robert Atkinson, Stress Analysis Dept., Northrop Aircraft, Inc.

Havens, Robert Fordham, B.Ae.E.; Jr. Aero. Engineer, Langley Mem. Aero. Lab., N.A.C.A.

Heimer, Harry James, S.B. in Ae.E.; Engineer, Douglas Aircraft Co.

Heinen, William P., Jr., B.Ae.E.; Jr. Aero. Engineer, Langley Mem. Aero. Lab., N.A.C.A.

Herrala, Carlo Oscar, Engineer (Mechanical), Boeing Aircraft Co.

Holt, Jack, M.E.; 2nd Lt., Planning & Inspection, Sacramento Air Depot, U.S. Army Air Corps.

Holtzclaw, Ralph Wayne, B.S. in Ae.E.; Jr. Aero. Engineer, Ames Aero. Lab., N.A.C.A.

Hood, Gordon Kay, Jr., B.S.E.; Stress Analyst, Bell Aircraft Corp.

Houck, Roy Mahaffey, B.S. in Ae.E.; Engineer, Airplane Div. (Columbus Plant), Curtiss-Wright Corp.

Hughes, Charles Samuel, B.S. in Ae.E.; Aviation Cadet, U.S. Navy.

Jobes, Harry William, B.Ae.E.; 2nd Lt., Corps of Engineers, U.S. Army.

Kane, Robert Frank, Meteorologist, Pan American Airways System.

Koellish, Wilfred, Draftsman, The Glenn L. Martin Co.

Koon, Charles Arnold, B.S. in M.E.; Draftsman, Boeing Aircraft Co.

Landis, Merle Anthony, B.Ae.E.; Aerodynamicist, Airplane Div. (Buffalo Plant), Curtiss-Wright Corp.

Laws, John Shields, B.M.E.; Aviation Cadet, U.S. Army Air Corps.

Le Roy, Warren Henry, Aero. Engineering Student, Tri-State College.

Levine, Arnold.

Light, James Albert, B.S. in M.E.; Instrument Inspector, Bendix Aviation Corp.

Lilligren, Robert Warren, B.Ae.E.; Engineering Trainee, Lockheed Aircraft Corp.

Lowell, Arthur Leon, 2nd Lt. U.S. Army Air Corps, Material Div., Wright Field.

Marchetti, Robert Mario, B.Ae.E.; Aerodynamics Dept., The Glenn L. Martin Co.

Marks, John Lewis, B.S. in Ae.E.

Mayer, Frank Stephan, Jr., S.B. in Ae.E.; Detail Draftsman, Consolidated Aircraft Corp.

Mills, Frank C., Jr., B.S. in M.E.; Supt. Aviation Training, Ground School, U.S. Naval Air Station, Pensacola.

Myers, Merrill Maitland, Engineer, Airplane Div. (Columbus Plant), Curtiss-Wright Corp.

Neff, Charles Warren, Inspector, Consolidated Aircraft Corp.

Neihouse, Abe David, B.S. in M.E.; Jr. Aero. Engineer, U.S. Marine Corps, Quantico, Va.

Nelson, Conrad Nathaniel, B.S. in Ae.E.; 2nd Lt., U.S. Army Air Corps, Wright Field.

Newby, Clinton Toms, M.S. in Ae.E.; Bureau of Aeronautics, Navy Dept.

Newman, Clark Leroy, Instructor, Educational Service Dept., Boeing School of Aeronautics.

O'Meara, Paul Weber, B.Ae.E.; Engineer (Stress), Airplane Div. (Buffalo Plant), Curtiss-Wright Corp.

Pamplin, Thomas N., B.S. in Ae.E.

Parr, John Marion, B.S. in G.E.; Liaison Draftsman, The Glenn L. Martin Co.

Petrey, Roger Aulis, M.E.; Stress Analysis Dept., North American Aviation, Inc.

Pinto, Albert Anthony, B.Ae.E.; Jr. Stress Analyst, The Glenn L. Martin Co.

Pritchard, George William, Aero. Engineer, The Glenn L. Martin Co.

Ranney, Daniel Rodier, B.S. in Ae.E.; Jr. Stress Analyst, The Glenn L. Martin Co.

Schaffer, David, B.S. in Ae.E.; Jr. Aero. Engineer, Langley Mem. Aero. Lab., N.A.C.A.

Schnaubelt, Norbert Cyril, Inspector, Consolidated Aircraft Corp.

Schunter, Hollis Harold, Asst. Meteorologist, Pan American Airways System.

Scott, John Frederick, B.S. in Ae.E.; Detail Draftsman, Consolidated Aircraft Corp.

Seamans, Robert Channing, Jr., B.S.; Research Asst., Mass. Inst. of Technology.

Simonds, Colwert Pier, Student Engineer & Asst. Inspector, Consolidated Aircraft Corp.

Smith, Richard Edgar, B.S. in M.E.; Detail Design Engineer, Boeing Aircraft Co.

Staros, Basil, S.B. in Ae.E.; Jr. Aero. Engineer, Material Div., U.S. Army Air Corps, Wright Field.

Stinson, Katharine, B.M.E.; Jr. Engineering Examiner, U.S. Civil Service Comm.

Strauss, Irvin Richard, Detail Engineer, Boeing Aircraft Co.

Tanaka, John Megumi, B.S. in Ae.E.; Draftsman, Aero. Labs., Univ. of Washington.

Thurlow, David Warren, Stress Analyst, Boeing Aircraft Co.

Troy, Leonard, B.S.E.; Stress Analyst & Design Engineer, Brewster Aeronautical Corp.

Tsu, Jack Chang-Nee, B.S. in Ae.E.

Tuttle, Roy Maynard, Jr., S.M. in Ae.E.; Aero. Structural Engineer, Vought-Sikorsky Aircraft Div., United Aircraft Corp.

Ullett, James Howard, Flying Cadet, U.S. Army Air Corps.

Wahle, Jack Arthur, B.S.; Apprentice Engineer, Pan American Airways System.

Walker, John Joseph, B.S. in M.E.; Engineering Trainee, Lockheed Aircraft Corp.

Walkowicz, Teddy Francis, S.B. in Ae.E.; 2nd Lt., Material Div., U.S. Army Air Corps, Wright Field.

Walling, Walter Charles, Research Assistant, New York University.

Weeber, Christian Gordon, B.S. in M.E.; Engineering Aide, Naval Aircraft Factory.

Westbrook, Charles Bevans, B.S.E.; 2nd Lt., Material Div., U.S. Army Air Corps, Wright Field.

Westfall, Vernon Dale, Layout Draftsman, Airplane Div. (Columbus Plant), Curtiss-Wright Corp.

Westvig, Roger Thomas, B.Ae.E.; Engineer (Stress), Goodyear Aircraft Corp.

Williams, Richard deHart, M.E.; Aerodynamicist, Boeing Aircraft Co.

Wilson, Robert Elmer, B.S. in G.E.

Wisken, Leonard James, Draftsman, Interstate Aircraft & Engineering Corp.

Wosika, Leon Rice, B.S. in Ae.E.; Engineer, Douglas Aircraft Co.

Wright, Fred Asbery, B.S. in M.E.; Draftsman (Hydraulics), Douglas Aircraft Co.